

New scalar resonances from sneutrino–Higgs mixing in supersymmetry with small lepton number (R-parity) violation

S. Bar-Shalom^a, G. Eilam^b and B. Mele^c

^a *Theoretical Physics Group, Rafael, Haifa 31021, Israel.**

^b *Physics Department, Technion-Institute of Technology, Haifa 32000, Israel.†*

^c *INFN, Sezione di Roma and Dept. of Physics, University of Roma I, La Sapienza, Roma, Italy.‡*
(October 25, 2018)

We consider new s -channel scalar exchanges in top quark and massive gauge-bosons pair production in e^+e^- collisions, in supersymmetry with a small lepton number violation. We show that a soft bilinear lepton number violating term in the scalar potential which mixes the Higgs and the slepton fields can give rise to a significant scalar resonance enhancement in $e^+e^- \rightarrow ZZ$, W^+W^- and in $e^+e^- \rightarrow t\bar{t}$. The sneutrino–Higgs mixed state couples to the incoming light leptons through its sneutrino component and to either the top quark or the massive gauge bosons through its Higgs component. Such a scalar resonance in these specific production channels cannot result from trilinear Yukawa-like R -parity violation alone, and may, therefore, stand as strong evidence for the existence of R -parity violating bilinears in the supersymmetric scalar potential. We use the LEP2 measurements of the WW and ZZ cross-sections to place useful constraints on this scenario, and investigate the expectations for the sensitivity of a future linear collider to these signals. We find that signals of these scalar resonances, in particular in top-pair production, are well within the reach of linear colliders in the small lepton number violation scenario.

PACS numbers: 12.60.Jv, 11.30.Fs, 14.80.Cp, 13.85.Lg

I. INTRODUCTION

Despite the enormous success of the Standard Model (SM), the SM spectrum and dynamics are believed to be the low energy limit of a more fundamental theory. There are, indeed, strong theoretical motivations for the existence of new physics above the electroweak mass scale: the mysterious large hierarchy from the electroweak scale to the Planck scale, the lack of a theory that unifies quantum physics with gravity, the observed dark matter in the universe etc...

One of the most favorable new physics candidates which may provide a viable framework for such questions is supersymmetry (SUSY). From the phenomenological point of view, SUSY offers some new attractive features which are absent in the SM and which may be tested in upcoming future colliders. One example of a fundamental difference between SUSY and the SM is associated with lepton number. In the SM lepton number must be conserved since it is not possible to write down a renormalizable lepton number violating interaction out of the SM fields. In SUSY, however, as opposed to the SM, lepton number does not have to be conserved since the most general set of SUSY renormalizable operators does allow for lepton number violating interactions. In particular, if one does not impose the so called R -parity symmetry [1] on the SUSY Lagrangian, then lepton number (and baryon number) can be violated at tree-level in interaction vertices involving both sparticles and particles.

Therefore, since there is no fundamental principle that enforces lepton number conservation, it is clear that lepton number violating phenomena should be explored in collider experiments even in processes not involving external SUSY partners. Such searches will provide an unambiguous test of the SM, and may give a first solid evidence about SUSY dynamics.

The SUSY R -parity conserving (RPC) superpotential can be written as (see e.g., [2] and references therein):

$$\mathcal{W}_{\text{RPC}} = \epsilon_{ab} \left[\frac{1}{2} h_{jk} \hat{H}_d^a \hat{L}_j^b \hat{E}_k^c + h'_{jk} \hat{H}_d^a \hat{Q}_j^b \hat{D}_k^c + h''_{jk} \hat{H}_u^a \hat{Q}_j^b \hat{U}_k^c - \mu_0 \hat{H}_d^a \hat{H}_u^b \right], \quad (1)$$

*e-mail: shaouly@physics.technion.ac.il

†e-mail: eilam@physics.technion.ac.il

‡e-mail: Barbara.Mele@roma1.infn.it

where $\hat{H}_u(\hat{H}_d)$ are the up(down)-type Higgs supermultiplet and $\hat{L}(\hat{E}^c)$ are the leptonic SU(2) doublet(charged singlet) supermultiplets. The \hat{Q} are quark SU(2) doublet supermultiplets and $\hat{U}^c(\hat{D}^c)$ are SU(2) up(down)-type quark singlet supermultiplets. Also, $j, k = 1, 2$ or 3 are generation labels and $a, b = 1, 2$ are SU(2) indices where ϵ_{ab} is the rank 2 anti-symmetric tensor.

If R-parity is violated, then lepton number may no longer be a conserved quantum number of the theory. In this case the \hat{L} and \hat{H}_d superfields, which have the same gauge quantum numbers, lose their identity since there is no additional quantum number that distinguishes between them. One can then construct additional renormalizable R-parity violating (RPV) interactions simply by replacing $\hat{H}_d \rightarrow \hat{L}$ in (1). Thus, the SUSY superpotential can violate lepton number (or more generally R-parity)¹ via an RPV Yukawa-like trilinear term (RPVTT) in the pure leptonic sector and via a mass-like RPV bilinear term (RPVBT) as follows [1]:²

$$\mathcal{W}_{RP, \mathcal{L}} \supset \epsilon_{ab} \left[\frac{1}{2} \lambda_{ijk} \hat{L}_i^a \hat{L}_j^b \hat{E}_k^c - \mu_i \hat{L}_i^a \hat{H}_u^b \right]. \quad (2)$$

Moreover, if R-parity is not conserved then, in addition to the usual RPC soft SUSY breaking terms, one must also add new trilinear and bilinear soft terms corresponding to the RPV terms of the superpotential, e.g., to the ones in (2). For our purpose, the relevant ones to be added to the SUSY scalar potential are the following soft breaking mass-like terms [3–5]:

$$V_{RPVBT} = (M_{LH}^2)_i \tilde{L}_i^a H_d^a - \epsilon_{ab} b_i \tilde{L}_i^a H_u^b, \quad (3)$$

where \tilde{L} and H_d are the scalar components of \hat{L} and \hat{H}_d , respectively.

The presence of such lepton number violating interactions in the SUSY Lagrangian drastically changes the phenomenology of SUSY. In general the new phenomenological implications of a RPV SUSY framework can be categorized according to the combinations of the RPV couplings involved. For example, one of the most interesting effects of the RPVTT in the superpotential is the possibility of having an s -channel sneutrino resonance formation in fermion pair production in leptonic colliders [6]. Such an effect will be proportional either to the product $\lambda\lambda$ (if a pair of leptons is produced) or to the product $\lambda\lambda'$ (if a pair of down-type quarks is produced), where λ and λ' are the trilinear RPV couplings in the superpotential (omitting subscripts), see Fig. 1(a). Among the interesting phenomenological implication associated with the RPVBT in the superpotential are tree-level neutrino masses [3,7,8] and flavor changing Z -decays (see e.g., Bisset *et al.*, in [8]); these effects are, therefore, proportional to the products $\mu\mu$ (omitting subscripts), where μ are the bilinear RPV couplings in the superpotential, see Fig. 1(b).

There are also new phenomena associated only with the soft RPVBT of the scalar potential, i.e., with the b terms in (3). Some examples for that are one-loop neutrino masses [3,5,9,10] and new scalar decay channels [11]. These will be proportional to the soft bilinear RPV coupling b and arise as a consequence of mixings in the scalar sector between the sleptons and the Higgs fields, see Fig. 1(c).

There are also RPV flavor changing phenomena in the SUSY fermionic sector such as rare leptonic Kaon decays and radiative muon decays, which are generated by the combined effect of the RPVTT and RPVBT in the superpotential [12]. These type of signals will be proportional to the products $\lambda\mu$ and/or $\lambda'\mu$, see Fig. 1(d).

In a previous paper [13] we have suggested yet a new type of signature of lepton number violation within SUSY, which is proportional to the product of the RPVTT coupling λ in the superpotential and the soft breaking RPVBT coupling b of the SUSY scalar potential, i.e., $\propto \lambda b$ - see Fig. 1(e). In particular, we have shown that one can have an observable scalar-resonance enhancement in the cross-section for producing a pair of massive gauge-bosons:

$$e^+e^- \rightarrow \Phi_{E,k} \rightarrow VV, \text{ with } V = W \text{ or } Z, \quad (4)$$

where $\Phi_{E,k}$, $k = 1, 2, 3$, are admixtures of the RPC CP-even neutral Higgs states and the sneutrino fields as described below.³

In this paper we wish to extend the analysis performed in [13] and, in addition, to investigate the effect of this type of RPV scalar resonances on top-quark pair production:

$$e^+e^- \rightarrow \Phi_{E,k}, \Phi_{O,\ell} \rightarrow t\bar{t}. \quad (5)$$

¹We will loosely refer to the SUSY interactions in (2) and (3) either as lepton number violating or RPV interactions.

²The lepton number violating RPVTT $\lambda' \hat{L} \hat{Q} \hat{D}^c$ is not relevant for our calculations.

³By an RPC state we mean the state in the RPC limit of $b_3 \rightarrow 0$.

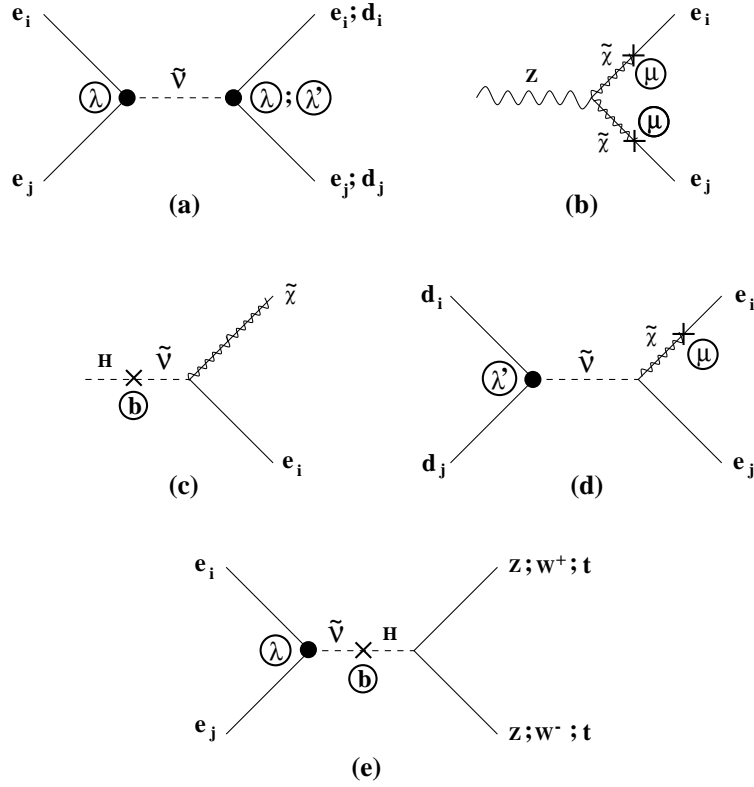


FIG. 1. Examples of RPV signals according to the combination of RPV couplings involved: (a) charged lepton or down-quark pair production through a sneutrino resonance in leptonic colliders $\propto \lambda\lambda$ or $\lambda\lambda'$, (b) leptonic flavor changing Z-decays, $Z \rightarrow e_i \bar{e}_j$, $\propto \mu\mu$, (c) RPV scalar (e.g., Higgs) decay through sneutrino-Higgs mixing, e.g., $H \rightarrow \tilde{\chi} e_i$ ($\tilde{\chi}$ =chargino), $\propto b$, (d) rare Kaon flavor changing leptonic decays, e.g., $K_L \rightarrow e_i \bar{e}_j$, $\propto \lambda'\mu$ and (e) the signal analyzed in this paper: s-channel scalar resonance in massive gauge-boson and top-quark pair production in leptonic colliders through sneutrino-Higgs mixing, $\propto \lambda b$.

The new resonance signal in top-quark pair production involves also s-channel exchanges of the CP-odd scalar states (i.e., of $\Phi_{O,\ell}$, $\ell = 1, 2, 3$, which are admixtures of the RPC CP-odd neutral Higgs and the CP-odd sneutrino fields), whereas in VV production only the CP-even admixtures (Φ_E) contribute since the CP-odd scalars do not couple to VV at tree-level [14].⁴

Such scalar resonances in top and massive gauge-boson pair production can arise with measurable consequences when the incoming e^+e^- beams couple to the sneutrino component in the new physical states, Φ_E or Φ_O , with a coupling $\lambda \gg m_e/M_W$ (that is the typical Higgs coupling to the incoming beams) in (2), while the VV and the $t\bar{t}$ final states couple to the Higgs components either in Φ_E or in Φ_O . Then, a non-vanishing scalar resonance in $e^+e^- \rightarrow VV$ and $e^+e^- \rightarrow t\bar{t}$ can be attributed to the Higgs-sneutrino mixing phenomena, and can serve as an exclusive probe of the soft breaking RPVBT in the SUSY scalar potential (i.e., of b). Indeed, the resonance effects are essentially proportional to the product λb which will vanish as $b \rightarrow 0$.

This differs from the situation of down-quark pair production via $e^+e^- \rightarrow \Phi_{E,k}, \Phi_{O,\ell} \rightarrow d\bar{d}$ ($d = d, s, b$) where the RPV scalar resonance may occur in two ways: (a) when the sneutrino component in Φ_E or in Φ_O couples to both the e^+e^- and $d\bar{d}$ through its trilinear RPV couplings λ and λ' , respectively (see e.g., [15] for a discussion of such a sneutrino resonance effect in $e^+e^- \rightarrow b\bar{b}$); (b) when the sneutrino component couples to e^+e^- then mixes with the Higgs state which couples to the $d\bar{d}$ final state. It is clear that in down quark pair production such a scalar resonance will be dominated by the purely RPVTT effect of type (a) above, as long as λ' is larger than the small Yukawa coupling of the neutral Higgs to down-quarks. In particular, an observable scalar resonance enhancement in $d\bar{d}$ production is possible even when $b \rightarrow 0$ and only the RPVTT contributes. On the other hand, in the $t\bar{t}$ production channel, the

⁴We note that the simultaneous presence of both CP-odd and CP-even scalar exchanges may give rise to interesting tree-level CP-violating effects in $e^+e^- \rightarrow t\bar{t}$. We do not discuss this possibility here.

purely RPVTT effect of type (1) above is absent at tree-level (the $t\bar{t}\tilde{\nu}$ coupling is forbidden by gauge-invariance). Similarly, there is no tree-level $VV\tilde{\nu}$ coupling when the soft breaking RPVBT vanishes, i.e., when $b \rightarrow 0$.

Thus, in contrast with down-quark and charged-lepton pair production in which a measurable scalar resonance enhancement is expected to emanate from the purely trilinear RPV couplings, in the channels considered here, the scalar resonance enhancement will arise only if the sneutrino and the Higgs states mix via the soft RPVBT. We therefore stress again that the scalar resonance formations in $t\bar{t}$ and VV production are fundamentally different from previously suggested sneutrino resonances in leptonic colliders within RPV SUSY (e.g., in fermion pair production [6]), since they are driven by RPV parameters from the soft breaking scalar sector and not purely by Yukawa-like RPV couplings from the superpotential. It should also be noted that the mechanism of a scalar resonance via sneutrino–Higgs mixing that we are considering here will not be efficient for light up-quark (i.e., u and c -quarks) pair production due to the smallness of the corresponding Higgs- u - \bar{u} and the Higgs- c - \bar{c} Yukawa couplings.

The paper is organized as follows: in Section II we define our low energy RPV SUSY framework and assumptions, we present the CP-even and CP-odd scalar mass matrices in the presence of the soft RPVBT and discuss their behavior in some limiting cases. In section III we derive the relevant Feynman rules for the new scalar mass-eigenstates and we calculate the cross-sections for the s -channel scalar exchanges in $e^+e^- \rightarrow ZZ$, WW and $e^+e^- \rightarrow t\bar{t}$. In section IV we present our numerical results for the expected resonance signals in $e^+e^- \rightarrow VV$, scanning the relevant SUSY parameter space at LEP2 and future linear colliders. In section V we investigate the sensitivity of future linear colliders to such scalar resonance signals in $e^+e^- \rightarrow t\bar{t}$. In section VI we present our conclusions.

II. NOTATIONS, ASSUMPTIONS AND FEATURES OF THE SNEUTRINO–HIGGS MIXING PHENOMENA

In what follows, for simplicity we will assume $b_i \neq 0$ only when $i = 3$ in (3), thus, considering only the mixing between the stau (\tilde{L}_3) and the Higgs scalar fields (H_d and H_u). The consequences of $b_1 \neq 0$ and/or $b_2 \neq 0$ is to introduce additional mixings among sleptons of different generations and mixings between the selectron and/or smuon with the Higgs fields which are not crucial for the main outcome of this paper.

The bilinear soft term b_3 leads in general to a non-vanishing VEV of the tau-sneutrino, $\langle \tilde{\nu}_3 \rangle = v_3 \neq 0$. However, since lepton number is not a conserved quantum number in this scenario, the \hat{H}_d and \hat{L}_3 superfields lose their identity and can be rotated to a particular basis (\hat{H}'_d, \hat{L}'_3) in which either μ_3 or v_3 are set to zero [3,7,5,9,10]. In what follows, we find it convenient to choose the “no VEV” basis, $v_3 = 0$, which simplifies our analysis below.

Furthermore, our key assumption will be that the lepton number violating couplings in the SUSY Lagrangian are small compared to the corresponding RPC ones wherever they appear. More specifically, the RPV parameters, λ and b_3 , will be limited such that $|\lambda_{ijk}| \leq 0.1$ and $b_3/b_0 \leq 0.1$. It is worth noting that the minimization of the scalar potential yields (in the $v_3 = 0$ basis) [3]: $b_3 = (M_{LH}^2 + \mu_3\mu_0)/t_\beta$, where $\tan\beta \equiv v_u/v_d$. Thus, in the general case, b_3 needs not vanish even if μ_3 is vanishingly small, as may be suggested by low energy flavor changing processes (see e.g., [12]) and flavor changing Z -decays (see e.g., Bisset *et al.*, in [8]). In particular, if $\mu_3 \rightarrow 0$ (so that $M_{LH}^2 \gg \mu_3\mu_0$) then $b_3 \sim M_{LH}^2/t_\beta$, in which case RPV in the scalar potential decouples from the RPV in the superpotential (i.e., b_3 is independent of μ_3). In such a case, small lepton number violation in the scalar potential should be realized by requiring only that $b_3 \ll b_0$.⁵ In this paper we will adopt this approach which treats RPV in the scalar potential independently from RPV in the superpotential.

Let us define the SU(2) components of the up and down neutral Higgs and tau-sneutrino scalar fields:⁶

$$\begin{aligned} H_u^0 &\equiv (\xi_u^0 + v_u + i\phi_u^0)/\sqrt{2}, \\ H_d^0 &\equiv (\xi_d^0 + v_d + i\phi_d^0)/\sqrt{2}, \\ \tilde{\nu}_\tau &\equiv (\tilde{\nu}_+^0 + v_3 + i\tilde{\nu}_-^0)/\sqrt{2}, \end{aligned} \tag{6}$$

where, as stated above, in the following discussion we always set $v_3 = 0$.

The CP-even and CP-odd 3×3 symmetric scalar squared-mass matrices M_E^2 and M_O^2 respectively, are then obtained through the quadratic part of the scalar potential:

⁵Note that the laboratory limit on the τ -neutrino mass allows $b_3/b_0 \sim \mathcal{O}(1)$ [5]

⁶We always use the superscript 0 to denote what would be the scalar states in the RPC limit $b_3 \rightarrow 0$.

$$\frac{1}{2} (\Phi_{E,O}^0)^T M_{E,O}^2 \Phi_{E,O}^0, \quad (7)$$

where

$$\Phi_E^0 = (\xi_d^0, \xi_u^0, \tilde{\nu}_+^0) \quad \text{and} \quad \Phi_O^0 = (\phi_d^0, \phi_u^0, \tilde{\nu}_-^0), \quad (8)$$

are the SU(2) weak states. The new CP-even and CP-odd scalar mass-eigenstates (i.e., the physical states) are derived by diagonalizing $M_{E,O}^2$. Let us denote the physical states by:

$$\Phi_E = (H, h, \tilde{\nu}_+) \quad , \quad \Phi_O = (A, G, \tilde{\nu}_-), \quad (9)$$

such that for small RPV in the SUSY Lagrangian, H , h and $\tilde{\nu}_+$ are the states dominated by the CP-even RPC states H^0 , h^0 and $\tilde{\nu}_+^0$, respectively, and A , $\tilde{\nu}_-$ are the states dominated by the CP-odd RPC states A^0 , $\tilde{\nu}_-^0$, respectively. Also, G is the Goldstone boson that is absorbed by the Z -boson and, therefore, is the state with a zero eigenvalue in M_O^2 .

Thus, the physical states $(\Phi_{E,O})$ are related to the weak eigenstates $(\Phi_{E,O}^0)$ via $\Phi_{E,O}^0 = S_{E,O} \Phi_{E,O}$, where $S_{E,O}$ are the rotation matrices that diagonalize $M_{E,O}^2$:

$$S_E^T M_E^2 S_E = \begin{pmatrix} m_H^2 & 0 & 0 \\ 0 & m_h^2 & 0 \\ 0 & 0 & (m_{s\nu}^+)^2 \end{pmatrix}, \quad (10)$$

$$S_O^T M_O^2 S_O = \begin{pmatrix} m_A^2 & 0 & 0 \\ 0 & 0 & 0 \\ 0 & 0 & (m_{s\nu}^-)^2 \end{pmatrix}. \quad (11)$$

As in (10) and (11) and throughout the rest of the paper, we will denote by $m_H, m_h, m_{s\nu}^+$ and $m_A, m_{s\nu}^-$ the masses of the CP-even and CP-odd physical states (when $b_3 \neq 0$), respectively. Similarly, adding the superscript 0, $m_H^0, m_h^0, m_{s\nu}^0, m_A^0$ will denote the corresponding masses in the RPC limit ($b_3 \rightarrow 0$). Note that in the RPC limit the CP-even and CP-odd tau-sneutrino states, $\tilde{\nu}_+^0$ and $\tilde{\nu}_-^0$, do not mix, and are, therefore, degenerate with a common mass $m_{\tilde{\nu}_+^0} = m_{\tilde{\nu}_-^0} \equiv m_{s\nu}^0$.

In the RPC limit the Higgs and sneutrino sectors decouple. That is, M_E^2 and M_O^2 consist of the usual 2×2 upper left blocks corresponding to the two CP-even and CP-odd Higgs states, respectively (which can be described at tree-level by only two parameters [16,17]) plus one sneutrino entry. The two Higgs parameters are conventionally chosen to be m_A^0 and $t_\beta \equiv \tan \beta$, where m_A^0 is related at tree-level to the soft bilinear mass term b_0 via $b_0 = (m_A^0)^2 c_\beta s_\beta$ ($s_\beta \equiv \sin \beta$ and $c_\beta \equiv \cos \beta$). Therefore, if the scalar potential conserves R-parity, then M_E^2 and M_O^2 can be written (at tree-level) as [3,16,18]:

$$M_E^2(RPC) = \begin{pmatrix} (m_A^0)^2 s_\beta^2 + m_Z^2 c_\beta^2 & -[(m_A^0)^2 + m_Z^2] s_\beta c_\beta & 0 \\ -[(m_A^0)^2 + m_Z^2] s_\beta c_\beta & (m_A^0)^2 c_\beta^2 + m_Z^2 s_\beta^2 & 0 \\ 0 & 0 & (m_{s\nu}^0)^2 \end{pmatrix}, \quad (12)$$

$$M_O^2(RPC) = \begin{pmatrix} (m_A^0)^2 c_\beta^2 & (m_A^0)^2 c_\beta s_\beta & 0 \\ (m_A^0)^2 c_\beta s_\beta & (m_A^0)^2 s_\beta^2 & 0 \\ 0 & 0 & (m_{s\nu}^0)^2 \end{pmatrix}. \quad (13)$$

However, if lepton number is violated in the scalar potential through $b_3 \neq 0$, then M_E^2 and M_O^2 acquire non-zero off-diagonal $\xi_{d,u}^0 - \tilde{\nu}_+^0$ and $\phi_{d,u}^0 - \tilde{\nu}_-^0$ mixing entries, respectively (which are $\propto b_3$), while in the "no VEV" basis the pure 2×2 Higgs blocks remain unchanged [3]. In this case, M_E^2 and M_O^2 are given by:

$$M_E^2 = \begin{pmatrix} (m_A^0)^2 s_\beta^2 + m_Z^2 c_\beta^2 + \delta_{dd} & -[(m_A^0)^2 + m_Z^2] s_\beta c_\beta + \delta_{du} & b_3 t_\beta \\ -[(m_A^0)^2 + m_Z^2] s_\beta c_\beta + \delta_{du} & (m_A^0)^2 c_\beta^2 + m_Z^2 s_\beta^2 + \delta_{uu} & -b_3 \\ b_3 t_\beta & -b_3 & (m_{s\nu}^0)^2 \end{pmatrix}, \quad (14)$$

$$M_O^2 = \begin{pmatrix} (m_A^0)^2 c_\beta^2 & (m_A^0)^2 c_\beta s_\beta & b_3 t_\beta \\ (m_A^0)^2 c_\beta s_\beta & (m_A^0)^2 s_\beta^2 & b_3 \\ b_3 t_\beta & b_3 & (m_{s\nu}^0)^2 \end{pmatrix}. \quad (15)$$

In (14) we have symbolically added to the tree-level CP-even mass matrix M_E^2 the quantities δ_{dd} , δ_{du} and δ_{uu} which are the 1-loop corrections to the CP-even pure Higgs block, i.e., the (ξ_d^0, ξ_u^0) block. Indeed, in our numerical analysis we include in δ_{dd} , δ_{du} and δ_{uu} the dominant 1-loop corrections coming from the $t - \tilde{t}$ sector. Below we use the present LEP2 lower bound on m_h in order to place limits on our RPV parameter space. The higher order corrections to the tree-level CP-even Higgs sector are, therefore, essential in evaluating the true theoretical value of the light Higgs mass, m_h , since they can generate a significant deviation (up to 50%) to the tree-level value of m_h .

Let us further note the following:

- Above we have "traded" the RPC soft breaking bilinear mass term b_0 for the "bare" pseudo-scalar Higgs mass m_A^0 (i.e., what would have been the physical mass of the pseudo-scalar Higgs state if R-parity were conserved), by using the RPC tree-level relation $b_0 = (m_A^0)^2 s_\beta c_\beta$ which, for $t_\beta^2 \gg 1$, implies $(m_A^0)^2 \sim b_0 t_\beta$. As will be shown below, for small RPV ($b_3/b_0 \ll 1$), A^0 and the new pseudo-scalar mass-eigenstate A are almost degenerate (i.e., $m_A \sim m_A^0$) if no accidental mass degeneracy occurs. This clearly follows from our definition of quantities which are denoted with the superscript 0. Hence, with the assumption of small RPV (RPV/RPC $\ll 1$) m_A also scales as $(m_A)^2 \sim b_0 t_\beta$, for $t_\beta^2 \gg 1$. Without loss of generality we then set:

$$b_3 \equiv \varepsilon (m_A^0)^2 / t_\beta \sim \varepsilon m_A^2 / t_\beta, \quad (16)$$

such that the small lepton number violation in the scalar sector is parameterized by the dimensionless quantity $\varepsilon \sim b_3/b_0$. Then $\varepsilon \ll 1$ corresponds to $b_3 \ll b_0$.

- As can be seen from (14) and (15), as a result of $b_3 \neq 0$, the usual CP-even RPC Higgs states H^0 and h^0 ($m_{H^0} > m_{h^0}$) will acquire a small $\tilde{\nu}_+^0$ component and vice versa due to the non-zero $(M_E^2)_{13,23,31,32}$ elements. Similarly, due to $(M_O^2)_{13,23,31,32} \neq 0$, the RPC pseudo-scalar state A^0 will acquire a small $\tilde{\nu}_-^0$ component and vice versa.
- Setting $b_3 \equiv \varepsilon (m_A^0)^2 / t_\beta$, our relevant low-energy SUSY parameter space is fully determined at tree-level by the four parameters m_A^0 , $m_{s\nu}^0$, t_β and ε . In particular, these four parameters completely fix M_E^2 and M_O^2 at tree-level from which the CP-even and CP-odd rotation matrices S_E and S_O as well as the tree-level physical masses $m_{\Phi_{E,k}}$ and $m_{\Phi_{O,k}}$ are derived by the diagonalization procedure.

Assuming that ε is a small parameter, we solve the eigenvalues equations for M_E^2 and M_O^2 perturbatively up to the second order in ε . We can thus write the new (physical) mass-squared eigenvalues, $m_{\Phi_{E,k}}^2$ and $m_{\Phi_{O,k}}^2$, in terms of the corresponding eigenvalues in the RPC limit, $m_{\Phi_{E,k}^0}^2$ and $m_{\Phi_{O,k}^0}^2$, as follows:

$$m_{\Phi_{E,k}}^2 = m_{\Phi_{E,k}^0}^2 \left(1 + \varepsilon \delta_{E,k}^{(1)} + \varepsilon^2 \delta_{E,k}^{(2)} + \mathcal{O}(\varepsilon^3) \right), \quad (17)$$

$$m_{\Phi_{O,k}}^2 = m_{\Phi_{O,k}^0}^2 \left(1 + \varepsilon \delta_{O,k}^{(1)} + \varepsilon^2 \delta_{O,k}^{(2)} + \mathcal{O}(\varepsilon^3) \right). \quad (18)$$

We then find that $\delta_{E,k}^{(1)} = \delta_{O,k}^{(1)} = 0$ and

$$\delta_{E,k}^{(2)} \propto \left(\frac{m_A^0}{m_{\Phi_{E,k}^0}} \right)^2 \times \frac{(m_A^0)^2}{m_{\Phi_{E,k}^0}^2 - m_{\Phi_{E,\ell}^0}^2}; \quad k \neq \ell, \quad (19)$$

$$\delta_{O,k}^{(2)} \propto \left(\frac{m_A^0}{m_{\Phi_{O,k}^0}} \right)^2 \times \frac{(m_A^0)^2}{m_{\Phi_{O,k}^0}^2 - m_{\Phi_{O,\ell}^0}^2}; \quad k \neq \ell. \quad (20)$$

Thus, with $\varepsilon \ll 1$ (implying $b_3 \ll b_0$ and also $b_3 \ll (m_A^0)^2$), the mass shifts induced by the RPVBT in (3) are, at leading order, $\propto \varepsilon^2$ (see also [3]). It is evident from (19) and (20) that, as long as there are no accidental mass degeneracies among scalar states of the same CP property, these mass shifts will remain small for $\varepsilon \ll 1$. Hence, although we are using "bare" masses (i.e., the scalar masses in the RPC limit) as inputs, it should be kept in mind that the physical masses are slightly shifted if there are no mass degeneracies as illustrated next.

In Fig. 2 we plot the mass shifts in the pseudo-scalar states: $\Delta m_A \equiv m_A - m_A^0$, $\Delta m_{s\nu}^- \equiv m_{s\nu}^- - m_{s\nu}^0$ and the mass splitting between the two CP-even and CP-odd sneutrino states, $\Delta m_{s\nu}^\pm \equiv m_{s\nu}^+ - m_{s\nu}^-$, due to $\varepsilon \neq 0$. This is shown as a function of m_A^0 , for two representative values of the "bare" sneutrino mass $m_{s\nu}^0 = 200, 500$ GeV, for $\varepsilon = 0.1$ and

$\tan\beta = 3$ or 50 . As expected from (19) and (20), Δm_A and $\Delta m_{s\nu}^-$ increase with m_A^0 and are inversely proportional to $(m_{s\nu}^0 - m_A^0)$ (they change sign at the turning point $m_{s\nu}^0 = m_A^0$). Also, for $\varepsilon = 0.1$ and in the ranges of m_A^0 and $m_{s\nu}^0$ considered, $\Delta m_A/m_A^0$ and $\Delta m_{s\nu}^-/m_{s\nu}^0$ are typically at the level of a few percent for both a low and a high $\tan\beta$ scenario (even for almost degenerate m_A^0 and $m_{s\nu}^0$).

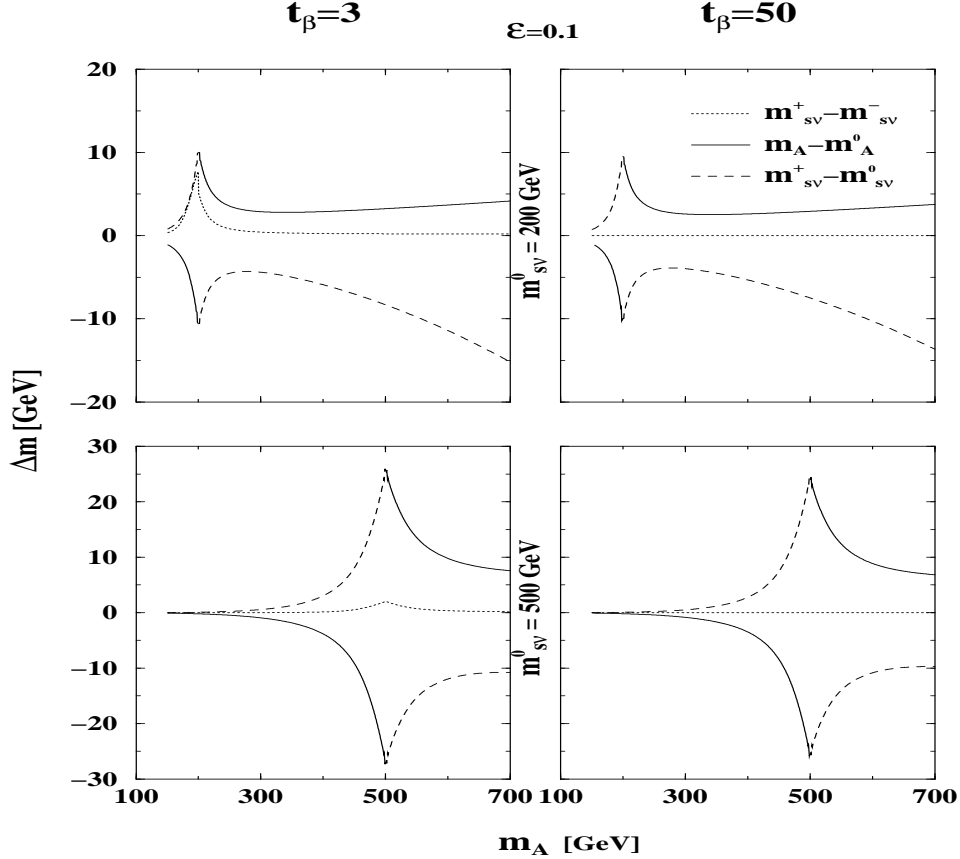


FIG. 2. The mass shifts $\Delta m_A \equiv m_A - m_A^0$, $\Delta m_{s\nu}^- \equiv m_{s\nu}^- - m_{s\nu}^0$ and the sneutrino mass splitting $\Delta m_{s\nu}^\pm \equiv m_{s\nu}^+ - m_{s\nu}^-$ induced by $\varepsilon = 0.1$, as a function of the RPC pseudo-scalar mass m_A^0 , for two values of the RPC sneutrino mass $m_{s\nu}^0 = 200$ and 500 GeV and for $t_\beta = 3$ (left figures) or $t_\beta = 50$ (right figures). See also text.

As for the sneutrino mass splitting $\Delta m_{s\nu}^\pm$, we see that a non-vanishing $\tilde{\nu}_+ - \tilde{\nu}_-$ mixing can occur only for a low $\tan\beta$ scenario, and when m_A^0 and $m_{s\nu}^0$ are sufficiently close. It should be noted that this sneutrino mixing phenomena can give rise to interesting lepton number violating effects such as radiative neutrino masses [9,10,19] and tree-level CP-violation in fermion pair production [20].

The behavior of the mass shifts in the CP-even sector, $\Delta m_{s\nu}^+ \equiv m_{s\nu}^+ - m_{s\nu}^0$ and $\Delta m_H \equiv m_H - m_H^0$, although not shown, is easily traced. Indeed, $\Delta m_{s\nu}^+$ may be inferred from the combination of $\Delta m_{s\nu}^-$ and $\Delta m_{s\nu}^\pm$ shown in Fig. 2: for very large $\tan\beta$ values, $\Delta m_{s\nu}^+ \sim \Delta m_{s\nu}^-$ whereas for smaller $\tan\beta$ values, $\Delta m_{s\nu}^+$ approaches $\Delta m_{s\nu}^-$ as m_A^0 is increased. In the case of the heavier CP-even Higgs, we find that $\Delta m_H \sim \Delta m_A$ in the decoupling limit where $(m_A^0)^2 \gg M_Z^2$, since then $m_H^0 \sim m_A^0$.

As mentioned above, due to the existing LEP2 lower bounds on the mass of the light CP-even Higgs, h , the mass shift $\Delta m_h = m_h - m_h^0$ caused by the RPBVT operator in (3), is crucial, since it determines the allowed range of our free parameter space $\{\varepsilon, m_A^0, m_{s\nu}^0, \tan\beta\}$ on which Δm_h depends. Moreover, the fact that the mass shifts in the CP-even sector are proportional to the sign of $(m_{\Phi_{E,k}^0} - m_{\Phi_{E,\ell}^0})$ has important consequences on the light CP-even Higgs particle. In particular, we find that if $m_A^0, m_{s\nu}^0 > m_{h^0}$ (as always chosen below), then m_h tends to decrease with ε . We can thus use the present LEP2 limit on m_h to deduce the allowed range in e.g., the $\varepsilon - m_{s\nu}^0$ plane, for a given m_A^0 (e.g., for $m_A \gtrsim 200$ GeV the present LEP2 bound is roughly $m_h \gtrsim 110$ GeV, irrespective of t_β and in the

maximal mixing scenario with a typical SUSY scale/squark mass of 1 TeV [21])⁷. Therefore, as mentioned earlier, we include the dominant higher order corrections (coming from the $t - \tilde{t}$ sector) to the (ξ_d^0, ξ_u^0) block in M_E^2 , which are denoted by δ_{uu}, δ_{dd} and δ_{du} in (14). To do that, we use the approximated formulae given in [18] with the maximal mixing scenario (as defined in [18]), and set the typical squark mass at $m_{\tilde{q}} \sim 1$ TeV.

In Fig. 3 we show the excluded region in the $\varepsilon - m_{sv}^0$ plane (the shaded area) from the recent LEP2 limit of $m_h \gtrsim 110$ GeV which holds for the parameters set $\tan \beta = 3$ or 50 and $m_A^0 = 300, 600$ or 900 GeV assumed in Fig. 3.

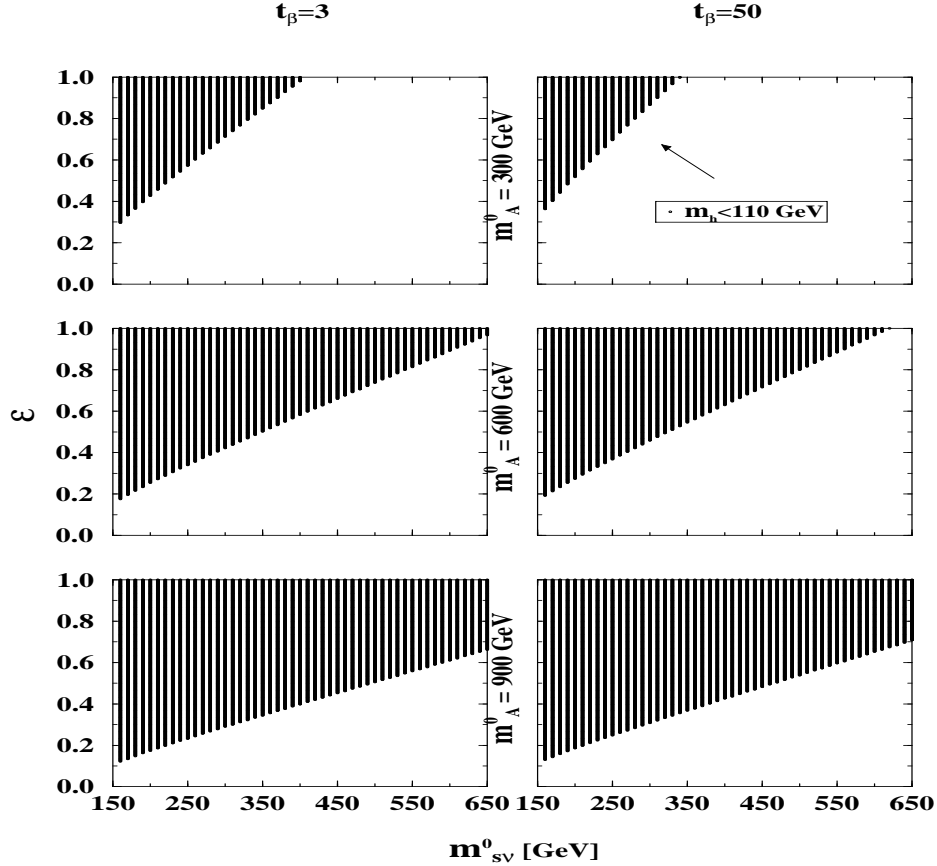


FIG. 3. The shaded areas in the $\varepsilon - m_{sv}^0$ plane [$\varepsilon \equiv b_3 t_\beta / (m_A^0)^2$] are excluded by the recent LEP2 limit on the light Higgs mass $m_h \gtrsim 110$ GeV. These excluded regions are given for $m_A^0 = 300, 600$ or 900 GeV, for $t_\beta = 3$ (left figures) or $t_\beta = 50$ (right figures) and are independent of the trilinear RPV coupling λ_{131} .

In what follows, in addition to our assumption of small RPV, we will focus on the case of a heavy Higgs spectrum (sometimes referred to as the decoupling limit) with $(m_A^0)^2 \gg M_Z^2$. As noted above, in this case there is a near mass degeneracy among the heavy CP-even Higgs and the pseudoscalar Higgs, $m_H^0 \sim m_A^0$ in the RPC limit. As shown in Fig. 2, as long as $\varepsilon \ll 1$, this near mass degeneracy will also hold among the corresponding new physical states, i.e., $m_H \sim m_A$.

Therefore, we wish to further investigate the behavior of the mixing matrices S_E and S_O under the three assumptions: (a) $\varepsilon \ll 1$ (small RPV in the scalar sector), (b) $(m_A^0)^2 \gg M_Z^2$ (heavy Higgs spectrum) and (c) $t_\beta^2 \gg 1$. In the small RPV scenario the elements of the CP-even and CP-odd mixing matrices, S_E and S_O , approach their RPC values:

$$S_E \xrightarrow{\varepsilon \rightarrow 0} S_E^0 = \begin{pmatrix} c_\alpha & -s_\alpha & 0 \\ s_\alpha & c_\alpha & 0 \\ 0 & 0 & 1 \end{pmatrix}, \quad (21)$$

⁷Since $b_3 \neq 0$ the hZZ coupling is smaller than its value in the RPC case leading to a smaller $e^+e^- \rightarrow Zh$ production rate. The limits on m_h given in [21] are therefore slightly weaker in the RPV case (see also [5]).

$$S_O \xrightarrow{\varepsilon \rightarrow 0} S_O^0 = \begin{pmatrix} s_\beta & -c_\beta & 0 \\ c_\beta & s_\beta & 0 \\ 0 & 0 & 1 \end{pmatrix}, \quad (22)$$

where S_E^0 and S_O^0 denote the corresponding CP-even and CP-odd scalar mixing matrices when R-parity is conserved. Also, $s_\alpha(c_\alpha) \equiv \sin \alpha(\cos \alpha)$ and α is the usual mixing angle of the RPC CP-even neutral Higgs sector defined through [2,16]:⁸

$$\tan 2\alpha = \tan 2\beta \frac{(m_A^0)^2 + M_Z^2}{(m_A^0)^2 - M_Z^2}. \quad (23)$$

Consider now the matrices S_E^0 and S_O^0 in the decoupling limit $(m_A^0)^2 \gg M_Z^2$. Since in this limit the heavier CP-even Higgs RPC state, H^0 , and the CP-odd RPC state, A^0 are almost degenerate, both H^0 and A^0 are considerably heavier than the Z -boson and, therefore, also heavier than the lighter CP-even Higgs state h^0 . In particular, when $(m_A^0)^2 \gg M_Z^2$ one obtains [17]:

$$\cos \alpha \xrightarrow{(m_A^0)^2 \gg M_Z^2} \sin \beta, \quad \sin \alpha \xrightarrow{(m_A^0)^2 \gg M_Z^2} -\cos \beta, \quad (24)$$

which in turn yields in the CP-even scalar sector:

$$S_E^0 \xrightarrow{(m_A^0)^2 \gg M_Z^2} \begin{pmatrix} s_\beta & c_\beta & 0 \\ -c_\beta & s_\beta & 0 \\ 0 & 0 & 1 \end{pmatrix}. \quad (25)$$

If in addition $t_\beta^2 \gg 1$, then it follows from (25) that:

$$\xi_d^0 \xrightarrow{\varepsilon \rightarrow 0} c_\alpha H - s_\alpha h \xrightarrow{(m_A^0)^2 \gg M_Z^2} s_\beta H + c_\beta h \xrightarrow{t_\beta^2 \gg 1} H, \quad (26)$$

$$\xi_u^0 \xrightarrow{\varepsilon \rightarrow 0} s_\alpha H + c_\alpha h \xrightarrow{(m_A^0)^2 \gg M_Z^2} -c_\beta H + s_\beta h \xrightarrow{t_\beta^2 \gg 1} h, \quad (27)$$

where now H and h are the physical states so that $H(h)$ is mostly composed out of the $\xi_d^0(\xi_u^0)$ weak state. Similarly, under $\varepsilon \ll 1$ and $t_\beta^2 \gg 1$, (22) will yield:

$$\phi_d^0 \xrightarrow{\varepsilon \rightarrow 0} s_\beta A - c_\beta G \xrightarrow{t_\beta^2 \gg 1} A, \quad (28)$$

$$\phi_u^0 \xrightarrow{\varepsilon \rightarrow 0} c_\beta A + s_\beta G \xrightarrow{t_\beta^2 \gg 1} G, \quad (29)$$

so that A is dominated by the ϕ_d^0 weak state.

For a summary of the notation introduced in this section for the various scalar states see Table I.

III. ANALYTICAL DERIVATION OF CROSS-SECTIONS

Let us denote the total cross-sections for $e^+e^- \rightarrow VV$ and $e^+e^- \rightarrow t\bar{t}$ by σ_V and σ_t respectively. In the presence of the RPV SUSY interactions in (2) and (3), new s -channel scalar exchanges have to be added at tree-level to the usual SM diagrams for these processes. The interferences between the SM diagrams and our s -channel scalar exchange diagrams (see Fig. 1(e)) are $\propto m_e$ and are therefore negligible. Thus, the total cross-sections above are given by the simple sums $\sigma_V = \sigma_V^{SM} + \sigma_V^s$ and $\sigma_t = \sigma_t^{SM} + \sigma_t^s$, where σ_V^s and σ_t^s are those parts of the cross-sections corresponding to the RPV scalar exchanges only:⁹

⁸Note that the 1-loop corrections to the pure Higgs block in the CP-even sector slightly shift the mixing angle, i.e., $\alpha \rightarrow \alpha'$. While these 1-loop effects are always included in our numerical analysis, for the purpose of understanding the qualitative features of the sneutrino-Higgs mixing phenomena it suffices to consider the tree-level values of M_E^2 . The small shift in α generates a significant effect only for the light CP-even Higgs h .

⁹Note that in [13] we used the superscript 0 to denote the scalar exchange cross-sections while here the superscript s is used instead.

Symbol	Particle/State it represents
H_u^0	Neutral field of the initial up-type Higgs SU(2) doublet
H_d^0	Neutral field of the initial down-type Higgs SU(2) doublet
$\tilde{\nu}_\tau$	Neutral field of the initial 3rd generation SU(2) slepton doublet
ξ_u^0	CP-even component of H_u^0
ϕ_u^0	CP-odd component of H_u^0
ξ_d^0	CP-even component of H_d^0
ϕ_d^0	CP-odd component of H_d^0
$\tilde{\nu}_+^0$	CP-even component of $\tilde{\nu}_\tau$, physical state when $b_3 = 0$
$\tilde{\nu}_-^0$	CP-odd component of $\tilde{\nu}_\tau$, physical state when $b_3 = 0$
Φ_E^0	CP-even weak states, $\Phi_E^0 = \xi_u^0, \xi_d^0$ or $\tilde{\nu}_+^0$
Φ_O^0	CP-odd weak states, $\Phi_O^0 = \phi_u^0, \phi_d^0$ or $\tilde{\nu}_-^0$
h^0	CP-even light Higgs, physical state when $b_3 = 0$
H^0	CP-even heavy Higgs, physical state when $b_3 = 0$
A^0	CP-odd Higgs, physical state when $b_3 = 0$
h	CP-even light Higgs, physical state for any (value of) b_3
H	CP-even heavy Higgs, physical state for any (value of) b_3
A	CP-odd Higgs, physical state for any (value of) b_3
G	CP-odd Goldstone boson
$\tilde{\nu}_+$	CP-even τ -sneutrino, physical state for any (value of) b_3
$\tilde{\nu}_-$	CP-odd τ -sneutrino, physical state for any (value of) b_3
Φ_E	CP-even physical states for any (value of) b_3 , $\Phi_E = H, h$ or $\tilde{\nu}_+$
Φ_O	CP-odd physical states for any (value of) b_3 , $\Phi_O = G, A$ or $\tilde{\nu}_-$

TABLE I. Notation used in this paper for the various physical (mass-eigenstates) scalar states and SU(2) (weak) scalar states.

$$\sigma_V^s \equiv \sigma(e^+e^- \rightarrow \Phi_E \rightarrow VV), \quad V = W \text{ or } Z, \quad (30)$$

$$\sigma_t^s \equiv \sigma(e^+e^- \rightarrow \Phi_E, \Phi_O \rightarrow t\bar{t}). \quad (31)$$

Recall that by Φ_E and Φ_O we mean $\Phi_E = H, h$ and $\tilde{\nu}_+$ and $\Phi_O = A$ and $\tilde{\nu}_-$ (the Goldstone boson G is not included) all of which has to be summed in the corresponding amplitudes. Note again that the CP-odd states Φ_O are absent in σ_V^s since they do not couple to VV at tree-level.

In order to calculate σ_V^s and σ_t^s we need the new Feynman rules for the vertices induced by the presence of the RPV SUSY terms. The interactions of the physical states Φ_E and Φ_O are obtained by rotating the Feynman rules of the RPC SUSY Lagrangian (see e.g., [2]) with the matrices S_E and S_O , respectively. Thus, if $\Lambda_{\Phi_{E,\ell}^0}$ is an interaction vertex involving the weak state $\Phi_{E,\ell}^0$ ($\ell = H^0, h^0$ or $\tilde{\nu}_+^0$), then $\Lambda_{\Phi_{E,k}}$ - the vertex involving the physical state $\Phi_{E,k}$ ($k = H, h$ or $\tilde{\nu}_+$) - is given by $\Lambda_{\Phi_{E,k}} = S_E^{\ell k} \Lambda_{\Phi_{E,\ell}^0}$. Similarly, in the CP-odd sector $\Lambda_{\Phi_{O,k}} = S_O^{\ell k} \Lambda_{\Phi_{O,\ell}^0}$, where now $\ell = A^0$ or $\tilde{\nu}_-^0$ and $k = A$ or $\tilde{\nu}_-$.

For the $\Phi_{E,k}VV$ coupling we then get:

$$\Lambda_{\Phi_{E,k}V_\mu V_\nu} = i(e/s_W)C_V m_V (c_\beta S_E^{1k} + s_\beta S_E^{2k}) g_{\mu\nu}, \quad (32)$$

where $C_V = 1(1/c_W)$ for $V = W(Z)$, $s_W(c_W) \equiv \sin \theta_W(\cos \theta_W)$ and $c_\beta(s_\beta) \equiv \cos \beta(\sin \beta)$.

The $\Phi_{E,k}t\bar{t}$ and $\Phi_{O,k}t\bar{t}$ couplings are:

$$\Lambda_{\Phi_{E,k}t\bar{t}} = -\frac{i}{2}(e/s_W)\frac{m_t}{M_W s_\beta} S_E^{2k}, \quad (33)$$

$$\Lambda_{\Phi_{O,k}t\bar{t}} = -\frac{1}{2}(e/s_W)\frac{m_t}{M_W s_\beta} S_O^{2k} \gamma_5. \quad (34)$$

The $\Phi_{E,k}e^+e^-$ and $\Phi_{O,k}e^+e^-$ couplings are obtained from the RPVTT term in (2). In particular, neglecting the Higgs couplings to electrons, only the couplings $\Lambda_{\tilde{\nu}_+^0 e^+e^-} = i\lambda_{131}/\sqrt{2}$ and $\Lambda_{\tilde{\nu}_-^0 e^+e^-} = -\lambda_{131}\gamma_5/\sqrt{2}$ need to be rotated (recall that $\tilde{\nu}_\pm^0$ refers here only to the tau-sneutrino). We then get:

$$\Lambda_{\Phi_{E,k}e^+e^-} = \frac{i}{\sqrt{2}}\lambda_{131}S_E^{3k}, \quad (35)$$

$$\Lambda_{\Phi_{O,k}e^+e^-} = -\frac{1}{\sqrt{2}}\lambda_{131}S_O^{3k}\gamma_5. \quad (36)$$

The cross-sections in (30) and (31) are then readily calculated in the new RPV interaction basis and are given by:

$$\sigma_V^s = \delta_V C_V^2 \frac{\alpha}{128s_W^2} \frac{\beta_V(3-2\beta_V^2+3\beta_V^4)}{s(1-\beta_V^2)} \lambda_{131}^2 \times \left| \sum_{k=1}^3 S_E^{3k} A_V^k \hat{\Pi}_E^k \right|^2, \quad (37)$$

and

$$\sigma_t^s = \frac{3\alpha}{32s_W^2} \left(\frac{m_t}{M_W s_\beta} \right)^2 \frac{\beta_t}{s} \lambda_{131}^2 \left\{ \left| \sum_{k=1}^3 S_O^{3k} S_O^{2k} \hat{\Pi}_O^k \right|^2 + \beta_t^2 \left| \sum_{k=1}^3 S_E^{3k} S_E^{2k} \hat{\Pi}_E^k \right|^2 \right\}, \quad (38)$$

where $\delta_V = 2(1)$ for $V = W(Z)$, $\beta_i = \sqrt{1-4m_i^2/s}$ and s is the square of the c.m. energy. We have further defined the "reduced" $\Phi_E^k VV$ coupling:

$$A_V^k \equiv c_\beta S_E^{1k} + s_\beta S_E^{2k}, \quad (39)$$

and the dimensionless propagator factors for the CP-even and CP-odd scalars:

$$\hat{\Pi}_{E,O}^k \equiv (1 - (x_{E,O}^k)^2 + i x_{E,O}^k y_{E,O}^k)^{-1}, \quad (40)$$

where

$$x_E^k, x_O^k \equiv \frac{m_{\Phi_{E,k}}; m_{\Phi_{O,k}}}{\sqrt{s}}, \quad y_E^k, y_O^k \equiv \frac{\Gamma_{\Phi_{E,k}}; \Gamma_{\Phi_{O,k}}}{\sqrt{s}}, \quad (41)$$

and $\Gamma_{\Phi_{E,k}}(\Gamma_{\Phi_{O,k}})$ is the $\Phi_{E,k}(\Phi_{O,k})$ width.

As mentioned before, in our numerical results we will evaluate σ_V^s and σ_t^s under the conditions of small RPV ($\varepsilon \ll 1$), a heavy Higgs spectrum ($(m_A^0)^2 \gg M_Z^2$, $t_\beta^2 \gg 1$ and that no accidental mass degeneracy between scalars of the same CP property occur. Under these assumptions it is possible to give a qualitative description of the behavior of σ_V^s and σ_t^s .

Let us consider first the cross-section σ_V^s . As was shown in the previous section, when $\varepsilon \ll 1$ and $(m_A^0)^2 \gg M_Z^2$ we have $S_E^{11} \rightarrow s_\beta$ and $S_E^{21} \rightarrow -c_\beta$ (see (21) and (25)), which therefore leads to $A_V^1 \rightarrow 0$, where A_V^1 is the reduced HVV coupling defined through (39). Moreover, for $\varepsilon \ll 1$, the element connecting H to $\tilde{\nu}_+^0$ diminishes, i.e., $S_E^{31} \ll 1$. Thus, the H exchange contribution to σ_V^s ($\propto \Lambda_{He^+e^-} \times \Lambda_{HVV} \sim S_E^{31} \times A_V^1$) is doubly suppressed.

As for the sneutrino-like state, $\tilde{\nu}_+$, due to $|(M_E^2)_{13}/(M_E^2)_{23}| = t_\beta$ (see (14)), $\tilde{\nu}_+^0$ acquires a larger ξ_d^0 mixing (as compared with ξ_u^0) which in turn implies a larger H mixing, since under the above conditions the H mass-eigenstate is mostly the ξ_d weak-state (see (26) and (27)). Therefore, the $\tilde{\nu}_+$ couples to the gauge-bosons pair mostly through its H component and $\Lambda_{\tilde{\nu}_+VV}$ and Λ_{HVV} get comparable (or equivalently $A_V^3 \sim A_V^1$). On the other hand, for $\varepsilon \ll 1$, $\tilde{\nu}_+$ has a much stronger (than H) coupling to the incoming electron since it couples to e^+e^- through its dominant $\tilde{\nu}_+^0$ component. In particular, $S_E^{33} \rightarrow 1$ as $\varepsilon \rightarrow 0$. Thus, even though $\Lambda_{\tilde{\nu}_+VV} \sim \Lambda_{HVV}$, the $\tilde{\nu}_+$ exchange contribution to σ_V^s , being $\propto S_E^{33} \times A_V^3$, will be much more pronounced than the H one, due to $S_E^{33} \gg S_E^{31}$.

Therefore, the more favorite scenario for observing such a sneutrino-Higgs mixing resonance in VV pair production is when the $\tilde{\nu}_+$ resonates. Note that a light Higgs (h) resonance in on-shell VV pair production is theoretically excluded, since the c.m. energy required to produce an on-shell VV pair is at least ~ 25 GeV above the highest possible m_h (the theoretical upper limit on m_h is ~ 135 GeV). Since we are only interested in the case of a sneutrino-Higgs resonance enhancement in σ_V^s , the h contribution which is always "far" from resonance is negligible - in particular near the $\tilde{\nu}_+$ resonance.

The case of s -channel scalar exchanges in $e^+e^- \rightarrow t\bar{t}$ is a little more complicated due to the extra CP-odd scalar exchanges in the s -channel. In the limit $(m_A^0)^2 \gg M_Z^2$ and $\varepsilon \ll 1$, we have $m_A \sim m_H$ and also $m_{s\nu}^+ \sim m_{s\nu}^-$ (see previous section). Therefore, if the $\tilde{\nu}_+$ resonates then necessarily also the $\tilde{\nu}_-$ will be close to resonance and is expected to yield a comparable enhancement in the vicinity of a $\tilde{\nu}_+$ resonance. Similarly, a H near-resonance enhancement will necessarily follow from an A resonance.

As it turns out, the situation here is similar to that in σ_V^s since here also the sneutrino-like states, $\tilde{\nu}_+$ and $\tilde{\nu}_-$, will potentially yield a stronger resonance enhancement than the Higgs-like states, H and A . This can be understood as follows. From (38) we see that, apart from the common factors that enter σ_t^s for each of the scalar states exchanges,

the relative strength between the A and $\tilde{\nu}_-$ contributions as well as between the H and the $\tilde{\nu}_+$ ones are determined by the quantities $S_O^{3k} \times S_O^{2k}$ and $S_E^{3k} \times S_E^{2k}$, respectively. Considering the cases $k = 1$ (the A and H exchanges) and $k = 3$ (the $\tilde{\nu}_-$ and $\tilde{\nu}_+$ exchanges), we have (see (21), (22) and (25)):

$$S_O^{31} \xrightarrow{\varepsilon \rightarrow 0} 0, \quad S_O^{33} \xrightarrow{\varepsilon \rightarrow 0} 1 \quad (42)$$

$$S_E^{31} \xrightarrow{\varepsilon \rightarrow 0} 0, \quad S_E^{33} \xrightarrow{\varepsilon \rightarrow 0} 1, \quad (43)$$

and

$$S_O^{21} \xrightarrow{\varepsilon \rightarrow 0} c_\beta \xrightarrow{t_\beta^2 \gg 1} 0, \quad S_O^{23} \xrightarrow{\varepsilon \rightarrow 0} 0 \quad (44)$$

$$S_E^{21} \xrightarrow{\varepsilon \rightarrow 0} s_\alpha \xrightarrow{m_A^2 \gg M_Z^2} -c_\beta \xrightarrow{t_\beta^2 \gg 1} 0, \quad S_E^{23} \xrightarrow{\varepsilon \rightarrow 0} 0. \quad (45)$$

Therefore, we see that also in the case of σ_t^s the sneutrino-like exchanges may potentially yield a stronger resonance when $\varepsilon \ll 1$, $m_A^2 \gg M_Z^2$ and $t_\beta^2 \gg 1$ since in this limit $S_O^{33} \times S_O^{23} \gg S_O^{31} \times S_O^{21}$ and $S_E^{33} \times S_E^{23} \gg S_E^{31} \times S_E^{21}$, mainly due to $S_O^{33} \gg S_O^{31}$ and $S_E^{33} \gg S_E^{31}$, respectively. Hence, since we are interested in the largest possible resonance enhancement in both $e^+e^- \rightarrow VV$ and $e^+e^- \rightarrow t\bar{t}$, in our numerical analysis we will investigate only the cases of resonances emanating from exchanges of the sneutrino-like admixtures while setting the masses of the Higgs-like states to be sufficiently away from the c.m. energy of the collider. In particular, in the VV production we will consider a resonance caused by the CP-even sneutrino-like state, $\tilde{\nu}_+$, and in $t\bar{t}$ production we will investigate the ‘‘combined’’ resonance effect that may emerge from the CP-odd and CP-even sneutrino states, $\tilde{\nu}_-$ and $\tilde{\nu}_+$. It should be clear, however, that if $m_A \sim m_{s\nu}^\pm$ (that will be the case for $\varepsilon \ll 1$ and if $m_A^0 \sim m_{s\nu}^0$), then both σ_V^s and σ_t^s may be further enhanced since there will be several scalar states whose masses are nearly degenerate and happen to lie close to the c.m. energy. In particular, under the conditions $(m_A^0)^2 \gg M_Z^2$ and $\varepsilon \ll 1$, choosing $m_A^0 \sim m_{s\nu}^0$ implies $m_{s\nu}^+ \sim m_{s\nu}^- \sim m_H \sim m_A$ in which case σ_V^s may exhibit a ‘‘double’’ resonance enhancement and σ_t^s may have a ‘‘four-fold’’ resonant structure. Here, we will not consider such a possibility of an accidental mass degeneracy among the scalar states involved which may give rise to these multi-resonant structures in σ_V^s and in σ_t^s .

Finally, the $\tilde{\nu}_\pm$ widths ($\Gamma_{\tilde{\nu}_\pm}$ in (41)) need to be included, since they crucially control the behavior of σ_V^s and of σ_t^s in the vicinity of our $\tilde{\nu}_+$ and $\tilde{\nu}_-$ resonances. Assuming that the lightest neutralino ($\tilde{\chi}_1^0$) is the Lightest SUSY Particle (LSP) and also that $m_{s\nu}^\pm > m_{\tilde{\chi}_1^+}$, where $\tilde{\chi}_1^+$ is the lighter chargino, then the RPC two-body decays $\tilde{\nu}_\pm \rightarrow \tilde{\chi}_1^0 \nu_\tau$, $\tilde{\chi}_1^+ \tau$ are open and dominate. Indeed, for $m_A^2 \gg M_Z^2$ and following the traditional assumption of an underlying grand unification with a common gaugino mass parameter $m_{1/2} < m_{s\nu}^0$, the mass hierarchy $m_{\tilde{\chi}_1^0} < m_{\tilde{\chi}_2^0} \sim m_{\tilde{\chi}_1^+} < m_{s\nu}^0$ and $m_{\tilde{\chi}_{3,4}^0} \sim m_{\tilde{\chi}_2^+} > m_{s\nu}^0$ is possible, e.g., when $m_{s\nu}^\pm < m_A$ [17] (recall that in the case of interest, $\varepsilon \ll 1$, we have $m_{s\nu}^0 \sim m_{s\nu}^+ \sim m_{s\nu}^-$, see previous section). Thus, upon ignoring phase space factors, a viable conservative estimate is (see e.g., Barger *et al.* in [6] and [22]): $\Gamma_{\tilde{\nu}_\pm} \sim \Gamma(\tilde{\nu}_\pm \rightarrow \tilde{\chi}_{1,2}^0 \nu_\tau) + \Gamma(\tilde{\nu}_\pm \rightarrow \tilde{\chi}_1^+ \tau) \sim 10^{-2} m_{s\nu}^\pm$ which we use below (for the ranges of ε , m_A^0 and $m_{s\nu}^0$ considered the possible RPV decays are sufficiently smaller and $\Gamma_{\tilde{\nu}_\pm} \sim \Gamma_{\tilde{\nu}_\pm^0}$ since $S_E^{33}, S_O^{33} \rightarrow 1$). Also, for reasons explained above, Γ_H, Γ_A and Γ_h have a negligible effect on our $\tilde{\nu}_\pm$ resonances and are therefore neglected.

IV. SNEUTRINO-LIKE RESONANCE IN $e^+e^- \rightarrow VV$. NUMERICAL RESULTS

Before presenting our numerical results for σ_V^s we wish to note the following:

- Sufficiently away from threshold (which occurs at $\beta_V \rightarrow 1$), $\sigma_W^s / \sigma_Z^s \sim (\delta_W c_W^2 / \delta_Z) \times (M_Z / M_W)^2 \sim 2$ and, since typically $\sigma_W^{SM} / \sigma_Z^{SM} > 10$, the relative effect of the scalar exchange cross-section is more pronounced in the ZZ channel. Therefore, below we will present results mainly for the ZZ production case (for σ_Z^s). It should be kept in mind, however, that σ_W^s is roughly a factor of 2 larger than σ_Z^s and exhibits the same behavior as a function of the relevant RPV parameter space.
- As mentioned in the previous section, for $\varepsilon \ll 1$ and when $(m_A^0)^2 \gg m_Z^2$, we have $\Lambda_{hVV} \rightarrow 1$ and $\Lambda_{HVV} \rightarrow 0$. If in addition $t_\beta^2 \gg 1$, one has $\xi_d^0 \rightarrow H$ and $\xi_u^0 \rightarrow h$ so that in conjunction with $(\Lambda_{hVV} / \Lambda_{HVV}) \gg 1$ also gives $(\Lambda_{\xi_u^0 VV} / \Lambda_{\xi_d^0 VV}) \gg 1$. Therefore, since the $\tilde{\nu}_+^0 - \xi_u^0$ mixing decreases with $\tan \beta$ [i.e., $|(M_E^2)_{23}| = b_3 = \varepsilon(m_A^0)^2 / t_\beta$, see (14)], as t_β increases the sneutrino ‘‘prefers’’ to mix more with ξ_d^0 which has a suppressed coupling to VV in this limit. As a consequence, the $\tilde{\nu}_+$ resonance effect in σ_V^s drops with $\tan \beta$ in the limit of small

RPV and when $m_A^2 \gg M_Z^2$. In what follows we will choose the two values $t_\beta = 3$ and $t_\beta = 50$ representing low and high $\tan\beta$ scenarios, respectively (note that already with our low $\tan\beta$ value, $t_\beta = 3$, t_β^2 is about an order of magnitude larger than unity). Following the above reasoning, it should be clear from the outset that $\sigma_V^s(t_\beta = 3) \gg \sigma_V^s(t_\beta = 50)$.

In Figs. 4 and 5 we show σ_Z^s as a function of $m_{s\nu}^0$ for c.m. energies of $\sqrt{s} = 200$ and 500 GeV, respectively. This is shown for $t_\beta = 3, 50$ and for $m_A^0 = 300, 600, 900$ GeV. For definiteness we choose $\varepsilon = 0.01, 0.05$ or 0.1 and $\lambda_{131} = 0.1$.¹⁰ The SM cross-sections $\sigma_Z^{SM}(\sqrt{s} = 200 \text{ GeV}) \sim 1.29$ [pb] and $\sigma_Z^{SM}(\sqrt{s} = 500 \text{ GeV}) \sim 0.41$ [pb] are also shown by the horizontal thick solid lines.

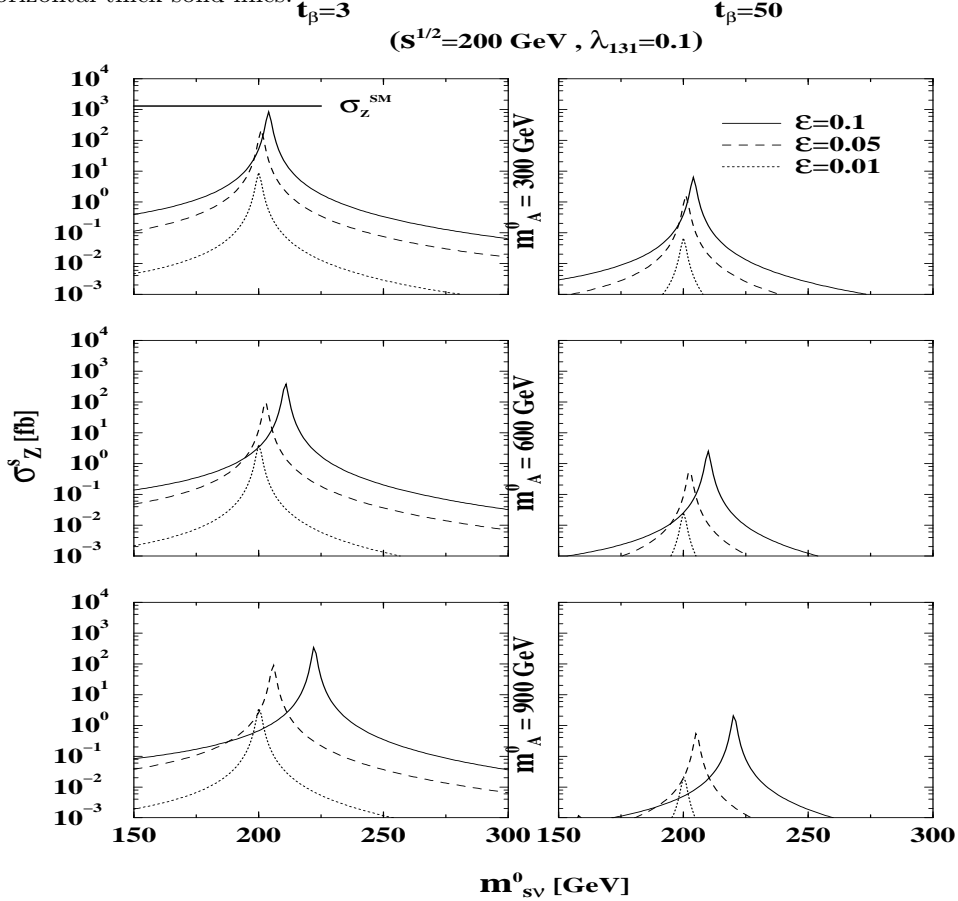


FIG. 4. σ_Z^s as a function of $m_{s\nu}^0$, for $m_A^0 = 300, 600$ and 900 GeV, for $t_\beta = 3$ (left figures) and $t_\beta = 50$ (right figures). For all combinations of m_A^0 and t_β values, σ_Z^s is shown for a c.m. energy of $\sqrt{s} = 200$ GeV with $\varepsilon = 0.1, 0.05$ and 0.01. Also, $\lambda_{131} = 0.1$ is used (recall that σ_Z^s scales as λ_{131}^2). The SM ZZ cross-sections for $\sqrt{s} = 200$ is also shown by the horizontal thick solid line.

As expected, σ_Z^s is larger for a smaller $|m_A^0 - m_{s\nu}^0|$ mass splitting since the sneutrino–Higgs mixing phenomena is proportional to $[(m_A^0)^2 - (m_{s\nu}^0)^2]^{-1}$ (see (19)). Clearly, the scalar exchange cross-section can be noticeable and statistically significant within some interval of $m_{s\nu}^+$ around the c.m. energy. As we shall see below, the interval $|m_{s\nu}^+ - \sqrt{s}|$ for which the RPV signal is statistically significant may range from a few GeV to a few tens of GeV depending on ε and the rest of the SUSY parameter space involved.

Let us first consider the case of \sqrt{s} around 200 GeV - that of LEP2 energies. We can use the measured values of the WW and ZZ cross-sections at LEP2 to place further bounds on the $\varepsilon - m_{s\nu}^0$ plane for a given m_A^0 and t_β . This is shown in Fig. 6 where we have taken the measured cross-sections σ_Z^{exp} and σ_W^{exp} (combined from the 4 LEP experiments) from the 183, 189, 192, 196, 200, 202, 205 and 207 GeV LEP2 runs as given in [23]. In particular, for

¹⁰ σ_V^s is insensitive to the signs of ε and λ_{131} .

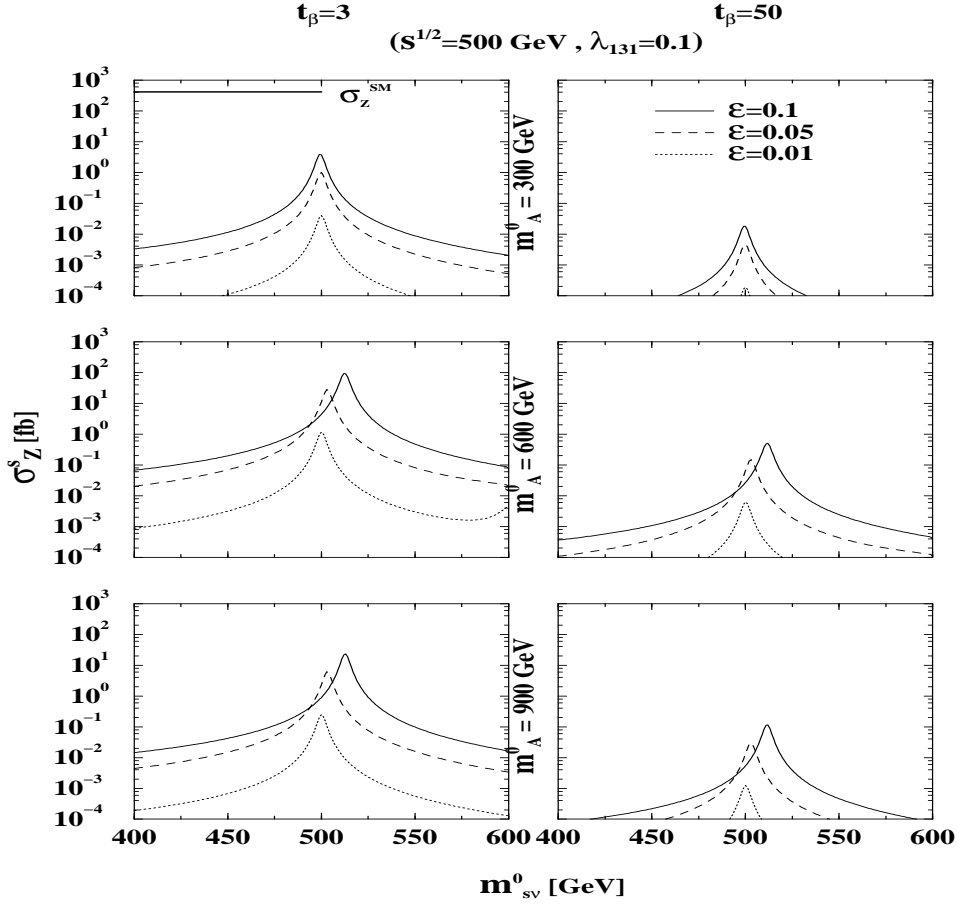


FIG. 5. Same as Fig. 4 but for a c.m. energy of 500 GeV.

each run we take the experimentally measured ($\sigma_V^{exp} \pm \Delta\sigma_V^{exp}$) and the SM theoretical ($\sigma_V^{SM} \pm \Delta\sigma_V^{SM}$) cross-sections (also given in [23]),¹¹ and require that:¹²

$$\sigma_V^s < (\sigma_V^{exp} - \sigma_V^{SM}) + \sqrt{(\Delta\sigma_V^{exp})^2 + (\Delta\sigma_V^{SM})^2} . \quad (46)$$

The 1σ excluded regions in Fig. 6 are derived through (46) for $\lambda_{131} = 0.1$ and for $t_\beta = 3$ with $m_A^0 = 300, 600$ or 900 GeV. For $t_\beta = 50$ and $m_A^0 \leq 300$ GeV we find that no such limits can be imposed since the RPV cross-sections σ_V^s are too small for such a large t_β value (we find a “tiny” excluded area in the $\varepsilon - m_{sv}^0$ plane for $t_\beta = 50$ and $m_A^0 = 300$ GeV and when $\varepsilon \gtrsim 0.15$).

Evidently, the limits coming from the ZZ and WW cross-sections measurements give further restrictions for $t_\beta = 3$ at low ε values (below ~ 0.2), in a sneutrino mass range of several tens of GeV¹³, for which there are no bounds coming from the LEP2 limits on m_h (see Fig. 3). Note that the fingers like shape of the shaded area in Fig. 6 is an artifact coming from the discrete set of c.m. energies used in accordance with the LEP2 runs.

Let us now examine the sensitivity of a future 500 GeV e^+e^- collider to the RPV sneutrino-like resonance effect in $e^+e^- \rightarrow VV$. We will require that our new RPV cross-section signal be smaller than the experimental error as in (46), where now all cross-sections are for a c.m. energy of 500 GeV. We will assume that the central value of the future measured cross-section for VV production at a c.m. energy of 500 GeV (σ_V^{exp}) coincides with the corresponding SM

¹¹For the ZZ and WW SM cross-sections we use the results of the ZZTO and YFSWW3 Monte-Carlos, respectively, where we take a 2% theoretical error for the ZZTO prediction and no error for the YFSWW3 one, see [23].

¹²Since σ_V^s always increases the SM cross-section, we do not include the cases in which $(\sigma_V^{exp} - \sigma_V^{SM}) + \sqrt{(\Delta\sigma_V^{exp})^2 + (\Delta\sigma_V^{SM})^2} < 0$.

¹³Note that, since $b_3 = \varepsilon(m_A^0)^2/t_\beta$, these 1σ limits can be directly translated into limits on the $b_3 - m_{sv}^0$ plane.

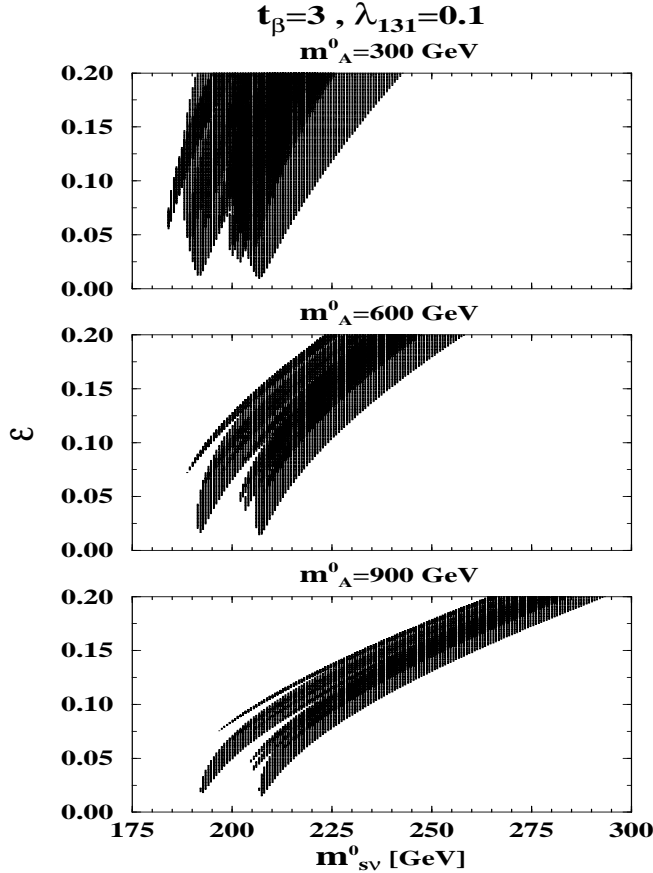


FIG. 6. 1σ excluded regions in the $\varepsilon - m_{s\nu}^0$ plane from the LEP2 measurements of the WW and ZZ cross-sections (see text), for $t_\beta = 3$ with $m_A^0 = 300, 600$ or 900 GeV and for $\lambda_{131} = 0.1$. Note that the fingers like shape of the shaded area is an artifact of the discrete set of *c.m.* energies used to derive these limits in accordance with the LEP2 runs.

theoretical value, i.e., $\sigma_V^{exp} = \sigma_V^{SM}$. Also, we combine the theoretical ($\Delta\sigma_V^{SM}$) and experimental ($\Delta\sigma_V^{exp}$) errors and scale it with the measured cross-section as follows:

$$\sqrt{(\Delta\sigma_V^{exp})^2 + (\Delta\sigma_V^{SM})^2} \equiv \sigma_V^{exp} \delta_V^\sigma = \sigma_V^{SM} \delta_V^\sigma, \quad (47)$$

such that δ_V^σ now represents the overall (statistical + systematic + theoretical) error per event [e.g., if $\Delta\sigma_V^{SM} \ll \Delta\sigma_V^{exp}$, then $\delta_V^\sigma = 0.1$ corresponds to a 10% error in the actual measurement of $\sigma(e^+e^- \rightarrow VV)$]. Thus, the condition for the observability of σ_V^s reduces to (at the 1σ level):

$$\frac{\sigma_V^s}{\sigma_V^{SM}} > \delta_V^\sigma. \quad (48)$$

Using (48), we can calculate the sneutrino-like mass range for which its contribution to the WW and ZZ cross-sections becomes observable (at 1σ). For example, if $\sigma(e^+e^- \rightarrow ZZ)$ is measured at a 500 GeV collider with an overall 5% or 10% error (i.e., $\delta_Z^\sigma = 0.05$ or 0.1), then, for $m_A^0 = 600, t_\beta = 3$ and $\varepsilon = \lambda_{131} = 0.1$, the scalar resonance signal in ZZ production will be observable within the sneutrino-like mass intervals $495 \text{ GeV} \lesssim m_{s\nu}^+ \lesssim 504 \text{ GeV}$ or $497 \text{ GeV} \lesssim m_{s\nu}^+ \lesssim 502 \text{ GeV}$, respectively. These mass ranges are further enlarged if an angular cut on the *c.m.* scattering angle, θ , is imposed, due to the different angular dependence of the signal and SM background. For example, with $-0.5 \lesssim \cos\theta \lesssim 0.5$, we find that the corresponding mass intervals are $490 \text{ GeV} \lesssim m_{s\nu}^+ \lesssim 509 \text{ GeV}$ for $\delta_Z^\sigma = 0.05$ and $494 \text{ GeV} \lesssim m_{s\nu}^+ \lesssim 507 \text{ GeV}$ for $\delta_Z^\sigma = 0.1$.

For the WW production case, with the angular cut $0 \lesssim \cos\theta \lesssim 1$ and for the same values of $t_\beta, m_A^0, \varepsilon$ and λ_{131} as above, the corresponding mass intervals are $494 \text{ GeV} \lesssim m_{s\nu}^+ \lesssim 506 \text{ GeV}$ for $\delta_W^\sigma = 0.05$ and $496 \text{ GeV} \lesssim m_{s\nu}^+ \lesssim 504 \text{ GeV}$ for $\delta_W^\sigma = 0.1$.

In the next section we will show that a much stronger RPV scalar resonance enhancement is expected in the reaction $e^+e^- \rightarrow t\bar{t}$.

V. SNEUTRINO-LIKE RESONANCE IN $e^+e^- \rightarrow t\bar{t}$. NUMERICAL RESULTS

As explained in section 3, We will mainly focus below on the case of a combined $\tilde{\nu}_- - \tilde{\nu}_+$ resonance in σ_t^s since those are expected to yield the largest possible scalar-resonance signal in $e^+e^- \rightarrow t\bar{t}$. Recall that $\varepsilon \ll 1$ implies a small $\tilde{\nu}_- - \tilde{\nu}_+$ mixing so that if one of the sneutrino-like states resonates so does the other which has an opposite CP property.

The $\tilde{\nu}_-$ and $\tilde{\nu}_+$ states couple to the top-quark through their ϕ_u^0 and ξ_u^0 components (the CP-odd and CP-even H_u^0 states, respectively, see (6)). Since the RPV $\tilde{\nu}_-^0 - \phi_u^0$ and $\tilde{\nu}_+^0 - \xi_u^0$ mixings are proportional to $b_3 = \varepsilon(m_A^0)^2/t_\beta$ (see $(M_O^2)_{23}$ and $(M_E^2)_{23}$ in (15) and (14)) and since the $\phi_u^0 t\bar{t}$ and $\xi_u^0 t\bar{t}$ couplings themselves also go like $1/t_\beta$, the $\tilde{\nu}_- t\bar{t}$ and $\tilde{\nu}_+ t\bar{t}$ couplings drop with t_β and we expect σ_t^s to significantly decrease as t_β is increased. Nonetheless, in most instances below we will present our numerical results again for the two values $t_\beta = 3$ and $t_\beta = 50$ in order to illustrate this behavior of σ_t^s as a function of t_β .

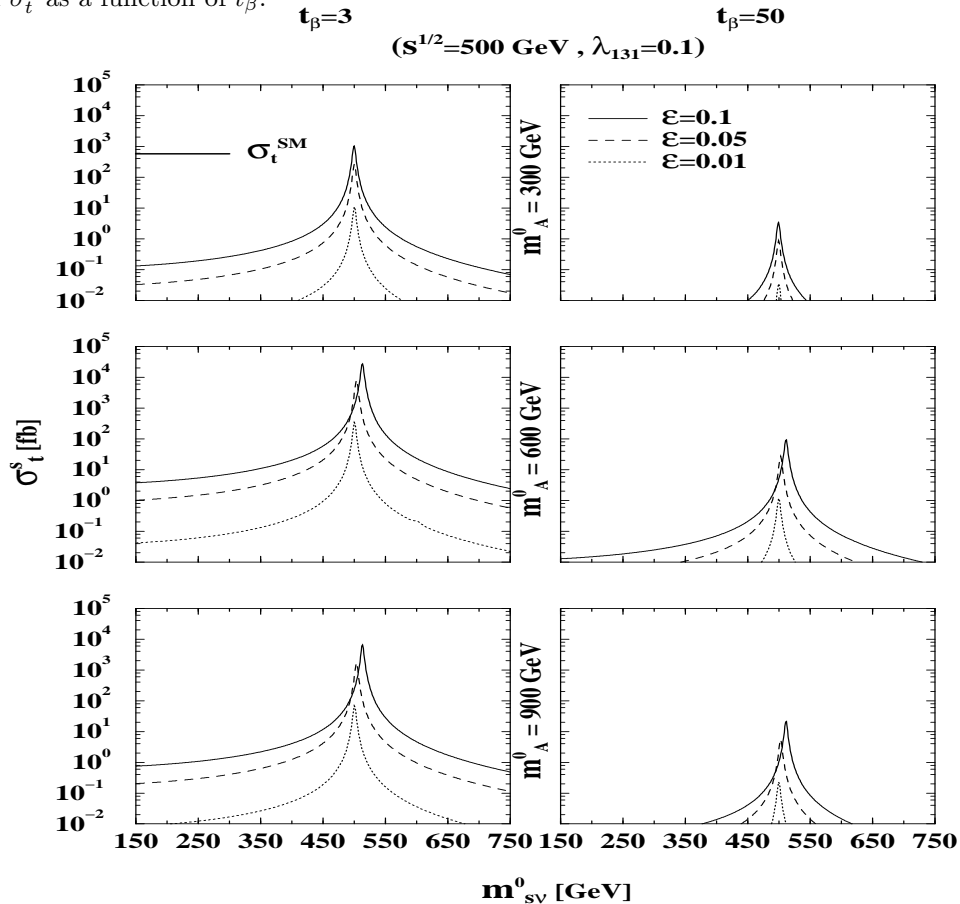


FIG. 7. σ_t^s as a function of m_{sv}^0 , for $m_A^0 = 300, 600$ and 900 GeV, for $t_\beta = 3$ (left figures) and $t_\beta = 50$ (right figures). For all combinations of m_A^0 and t_β values, σ_t^s is shown for a c.m. energy of $\sqrt{s} = 500$ and with $\varepsilon = 0.1, 0.05$ and 0.01 . Also, $\lambda_{131} = 0.1$ is used (recall that σ_t^s scales as λ_{131}^2). The SM $t\bar{t}$ cross-section for $\sqrt{s} = 500$ is also shown by the horizontal thick solid line.

In Figs. 7 we plot σ_t^s as a function of m_{sv}^0 for an e^+e^- collider with a c.m. energy of 500 GeV. This is shown for $t_\beta = 3, 50$ and for $m_A^0 = 300, 600$ or 900 GeV. The RPV couplings are set to $\varepsilon = 0.01, 0.05$ or 0.1 and $\lambda_{131} = 0.1$.¹⁴ The SM cross-section $\sigma_t^{SM}(\sqrt{s} = 500 \text{ GeV}) \sim 580$ [fb] is also shown by the horizontal thick solid line.

In Figs. 8 we show σ_t^s as a function of the c.m. energy, \sqrt{s} , ranging from the $t\bar{t}$ threshold to 750 GeV. Here we fixed the RPV couplings to be $\varepsilon = \lambda_{131} = 0.1$ and we depicted σ_t^s for combinations of $t_\beta = 3, 50$ with $m_A^0 = 300$ or

¹⁴ σ_t^s is also insensitive to the signs of ε and λ_{131} .

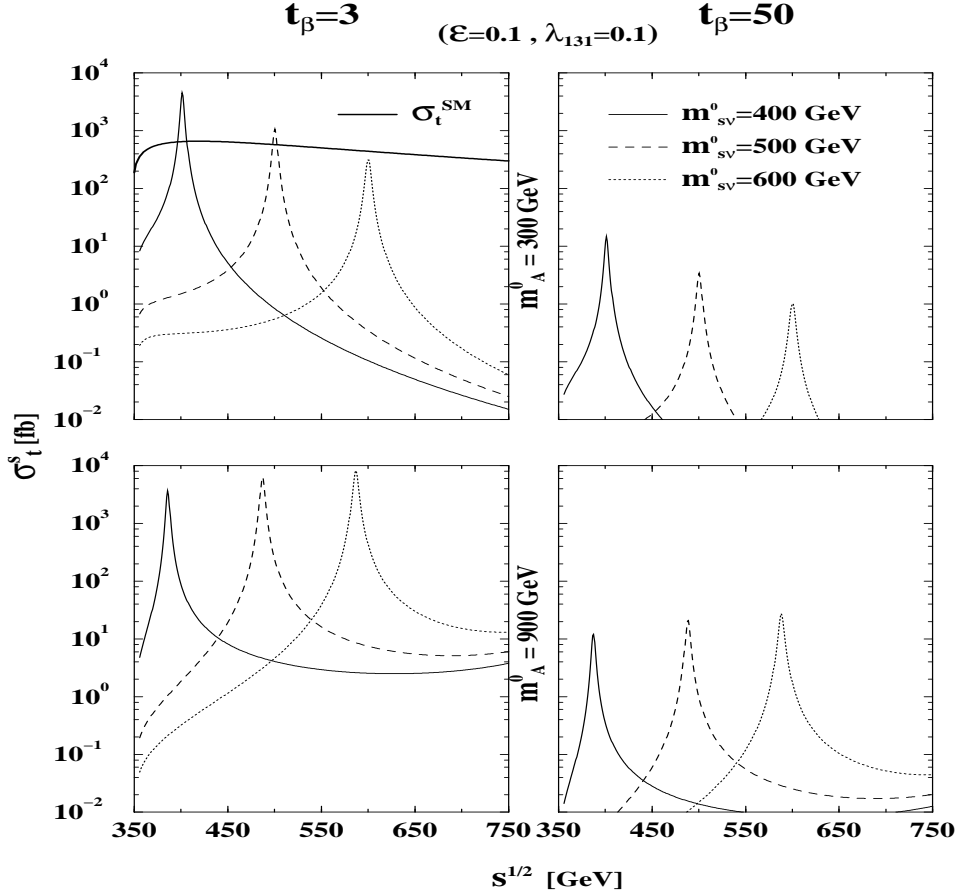


FIG. 8. σ_t^s as a function of the c.m. energy \sqrt{s} , for $m_A^0 = 300$ and 900 GeV and for $t_\beta = 3$ (left figures) or $t_\beta = 50$ (right figures). For all combinations of m_A^0 and t_β values σ_t^s is shown for $\varepsilon = 0.1 = \lambda_{131} = 0.1$ and for $m_{s\nu}^0 = 400, 500$ and 600 GeV. The SM $t\bar{t}$ cross-section is also shown by the thick solid line. See also caption to Fig. 7.

900 GeV, where our input sneutrino mass (i.e., in the RPC limit) was given three values: $m_{s\nu}^0 = 400, 500$ and 600 GeV. The SM $t\bar{t}$ production cross-section, σ_t^{SM} is again shown by a thick solid line.

From Figs. 7 and 8 it is evident that the scalar exchange cross-section σ_t^s decreases significantly as t_β is increased. Also here, as expected, σ_t^s is larger for a smaller $|m_A^0 - m_{s\nu}^0|$ mass splitting, due to factors of $[(m_A^0)^2 - (m_{s\nu}^0)^2]^{-1}$ which enter the mixing matrices S_O and S_E in σ_t^s (see section 3).

Evidently, the scalar exchange contribution in $e^+e^- \rightarrow t\bar{t}$ can be statistically significant within a rather large mass range of $m_{s\nu}^-$ and $m_{s\nu}^+$ around resonance. As we shall see below, the interval $|m_{s\nu}^- - \sqrt{s}|$, for which this RPV resonance signal may be observable in $t\bar{t}$ production in a future e^+e^- high energy collider can range from a few tens of GeV up to more than a hundred GeV, depending on theoretical parameters such as $\varepsilon, \lambda_{131}$ and also on the precision that will be achieved in measuring observable quantities.

Let us investigate more quantitatively the limits that can be placed on this RPV scalar mixing scenario in case that no such resonant enhancement will be detected in $e^+e^- \rightarrow t\bar{t}$ at a 500 GeV e^+e^- machine. To estimate that, we require again that our new RPV cross-section signal be smaller than the experimental error as in (46). Here also, we assume that the central value of the future measured cross-section for $t\bar{t}$ production at a c.m. energy of 500 GeV (σ_t^{exp}) coincides with the corresponding SM theoretical value, i.e., $\sigma_t^{exp} = \sigma_t^{SM}$, and we combine the theoretical ($\Delta\sigma_t^{SM}$) and experimental ($\Delta\sigma_t^{exp}$) errors to scale with the measured cross-section as in (47). Then, the condition for observability of σ_t^s (at the 1σ level) becomes (see also (48)):

$$\frac{\sigma_t^s}{\sigma_t^{SM}} > \delta_t^\sigma. \quad (49)$$

As an example, using (49) we find that if the $t\bar{t}$ production cross-section is measured with an overall 10% error ($\delta_t^\sigma = 0.1$), then, for $t_\beta = 3$ and $\varepsilon = \lambda_{131} = 0.1$, one can exclude the sneutrino mass intervals $492 \text{ GeV} \lesssim m_{s\nu}^0 \lesssim 507 \text{ GeV}$, $463 \text{ GeV} \lesssim m_{s\nu}^0 \lesssim 560 \text{ GeV}$ and $492 \text{ GeV} \lesssim m_{s\nu}^0 \lesssim 534 \text{ GeV}$ for $m_A^0 = 300, 600$ and 900 GeV, respectively. In terms

of the masses of the physical states $\tilde{\nu}_+$ and $\tilde{\nu}_-$ (recall that $m_{s\nu}^- \sim m_{s\nu}^+$ for $\varepsilon = 0.1$, see Fig. 2) the above excluded mass ranges remain roughly the same, however, centered around ~ 500 GeV.

Asymmetries are often better probes of new physics since they involve ratios of cross-sections. From the experimental point of view, ratios of cross-sections can be determined with larger accuracy since their systematic errors are usually in better control compared to “simple” cross-sections measurements. We therefore expect asymmetries such as the Forward-Backward (FB) asymmetry:

$$A_{FB} \equiv \frac{\int_0^{\pi/2} \{d\sigma(\theta) - d\sigma(\pi - \theta)\}}{\sigma}, \quad (50)$$

to be more sensitive to our new RPV scalar resonance effect in $e^+e^- \rightarrow t\bar{t}$ due to the better accuracy with which it can be measured.

In general, an s -channel scalar exchange does not have a FB asymmetry since the corresponding cross-section (in our case σ_t^s or σ_V^s) does not depend on θ . In any given process for which there exists a non-vanishing FB asymmetry within the SM, such a scalar exchange will reduce its SM (absolute) value since it will make no contribution to the numerator of (50) while increasing the total cross-section and therefore the denominator in (50). In top pair production various types of asymmetries can be constructed, e.g., polarization asymmetries, FB asymmetries and also combinations of these two. Here we consider only the simplest FB asymmetry for unpolarized top quarks and unpolarized incoming electron beams as in (50). The RPV s -channel scalar exchanges in $e^+e^- \rightarrow t\bar{t}$ will alter the SM FB asymmetry as follows:

$$A_{FB(t)}^{SM} \rightarrow A_{FB(t)}^{RPV} = A_{FB(t)}^{SM} \times \left(1 + \frac{\sigma_t^s}{\sigma_t^{SM}}\right)^{-1}. \quad (51)$$

In Fig. 9 we plot the FB asymmetry $A_{FB(t)}^{RPV}$ as a function of the “bare” sneutrino mass $m_{s\nu}^0$ for a 500 GeV collider, for $t_\beta = 3$ or $t_\beta = 50$ with $m_A^0 = 300, 600$ or 900 GeV. The FB asymmetry is shown for $\lambda_{131} = 0.1$ with three values of the RPV scalar mixing parameter, $\varepsilon = 0.1, 0.05$ and 0.01 . Only low t_β values can give rise to a significant shift from the SM FB asymmetry in $t\bar{t}$ production (the very small shifts in the case of $t_\beta = 50$ are barely noticeable on the scale used in Fig. 9). We see that these deviations from $A_{FB(t)}^{SM}$ can be remarkable, reaching several tens of percent in a rather large range of the sneutrino mass around 500 GeV.

We can, therefore, examine the expected limits on the sneutrino–Higgs mixing scenario that can be obtained purely from the FB asymmetry in $e^+e^- \rightarrow t\bar{t}$. We again assume that the central value of the future measured FB asymmetry in $t\bar{t}$ production (at a c.m. energy of 500 GeV) takes the value of the corresponding SM theoretical value, i.e., $A_{FB(t)}^{exp} = A_{FB(t)}^{SM}$, and that the combined overall experimental error is parametrized by the relative error δ_t^{FB} as:¹⁵

$$\Delta A_{FB(t)}^{exp} \equiv \delta_t^{FB} A_{FB(t)}^{exp} = \delta_t^{FB} A_{FB(t)}^{SM}, \quad (52)$$

such that $\delta_t^{FB} = 0.1$ implies a 10% accuracy in $A_{FB(t)}^{exp}$.

Then, the deviation in the FB asymmetry due to the RPV should be larger than the overall error $\Delta A_{FB(t)}^{exp}$

$$|A_{FB(t)}^{RPV} - A_{FB(t)}^{SM}| > \delta_t^{FB} A_{FB(t)}^{SM}. \quad (53)$$

In terms of the cross-sections (53) yields:

$$\frac{\sigma_t^s}{\sigma_t^{SM}} > \frac{\delta_t^{FB}}{1 - \delta_t^{FB}}. \quad (54)$$

Clearly, since δ_t^{FB} as well as δ_t^σ are smaller than one, the condition in (54) is stronger than the one obtained in (49) through the cross-section analysis when $\delta_t^{FB} = \delta_t^\sigma$. However, as mentioned above, if the FB asymmetry will be measured to a better accuracy than the cross-section, i.e., $\delta_t^{FB} < \delta_t^\sigma$, and no deviation from the SM is detected, then the limits obtained through (54) could be more stringent than the ones obtained through (49).

In Fig. 10 we show the sneutrino mass intervals that can be excluded for a given δ_t^{FB} in a measurement of the FB asymmetry in $e^+e^- \rightarrow t\bar{t}$ at a 500 GeV collider by requiring (54). The excluded mass intervals are plotted for the case $\varepsilon = \lambda_{131} = 0.1$, for $t_\beta = 3$ and for $m_A^0 = 300, 600$ or 900 GeV.

¹⁵Again we assume that $\Delta A_{FB(t)}^{SM} \ll \Delta A_{FB(t)}^{exp}$. Otherwise (52) should read: $\sqrt{(\Delta A_{FB(t)}^{exp})^2 + (\Delta A_{FB(t)}^{SM})^2} \equiv \delta_t^{FB} A_{FB(t)}^{exp} = \delta_t^{FB} A_{FB(t)}^{SM}$.

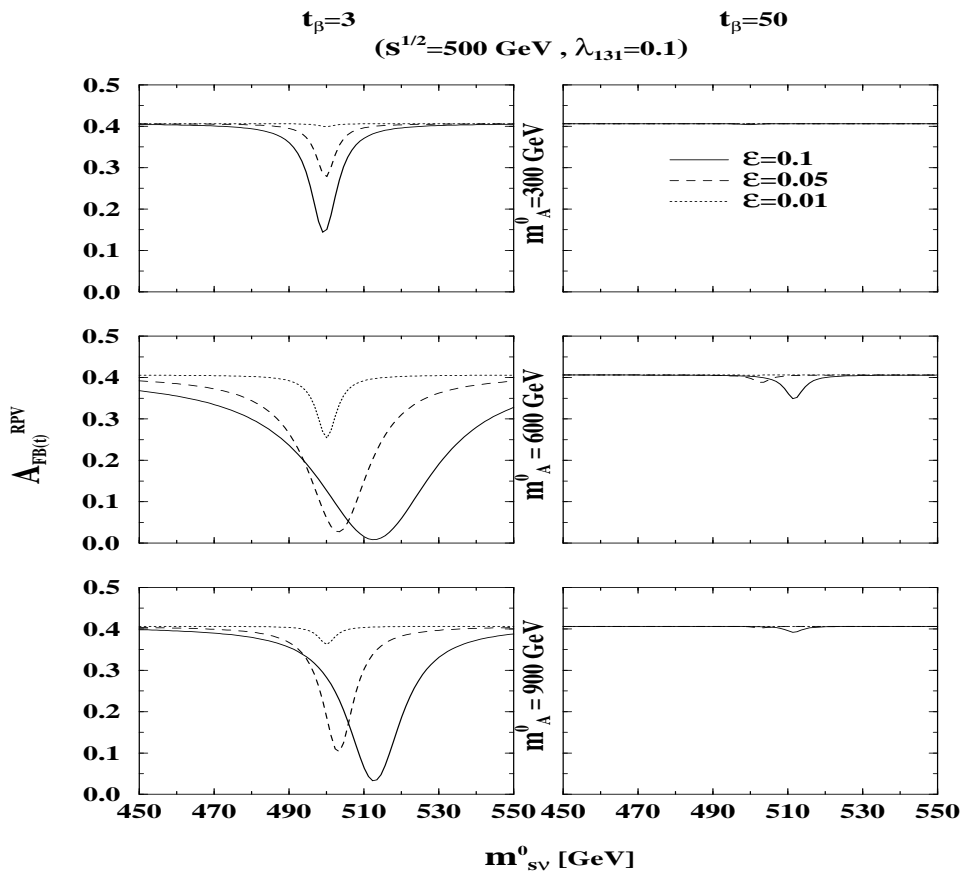


FIG. 9. The FB asymmetry $A_{FB(t)}^{RPV}$ defined in (51) as a function of the RPC sneutrino mass m_{sv}^0 in an e^+e^- collider running at a c.m. energy of $\sqrt{s} = 500$ GeV. The asymmetry is shown for $m_A^0 = 300, 600$ and 900 GeV and for $t_\beta = 3$ (left figures) or $t_\beta = 50$ (right figures). For all combinations of m_A^0 and t_β , $A_{FB(t)}^{RPV}$ is given for $\lambda_{131} = 0.1$ and for $\varepsilon = 0.1, 0.05$ or 0.01 . The corresponding SM value is $A_{FB(t)}^{SM} \sim 0.41$.

Clearly, the FB asymmetry is a powerful probe of this signal or, in case that no such signal is detected, is very useful in placing limits on this scenario. For example, if $A_{FB(t)}^{exp}$ is measured at a 500 GeV machine with an error not exceeding 5%, then a more than 100 GeV sneutrino mass interval can be excluded if no deviation from the SM is observed for $\varepsilon = \lambda_{131} = 0.1$, $t_\beta = 3$ and for $m_A^0 = 600$ GeV. At the same time, a deviation in the measured FB asymmetry will provide a candidate signal for the s -channel scalar exchanges driven by the sneutrino–Higgs mixing phenomena. Such additional signals beyond just resonance enhancement in the cross-section should help decipher the nature of the new physics involved. In particular, as can be seen from (51), a reduction (from the SM value) in the FB asymmetry should give further evidence for s -channel scalar exchanges which in turn should strengthen the theoretical possibility of the sneutrino–Higgs mixing via the lepton number violating RPVBT in (3).

On the other hand, it should be noted that in the ZZ/WW system the FB asymmetry is not as useful. In particular, in ZZ production $A_{FB(Z)}^{SM} = 0$ and, therefore, also $A_{FB(Z)}^{RPV} = 0$ [see (51) and replace the index t with Z]. In such a case case no further information can be gained from the FB asymmetry. The reaction $e^+e^- \rightarrow W^+W^-$ does, however, have a non-zero FB asymmetry within the SM and so the s -channel scalar exchanges will decrease the FB asymmetry from $A_{FB(W)}^{SM}$ to $A_{FB(W)}^{RPV}$ according to (51). Unfortunately, due to the much larger SM W^+W^- cross-section (as mentioned in the previous section $\sigma_W^s/\sigma_W^{SM} \ll \sigma_Z^s/\sigma_Z^{SM}$), the effect of the sneutrino-like resonance is too small to cause an appreciable shift to $A_{FB(W)}^{SM}$ as long as our dimensionless RPV parameters are kept below ~ 0.1 . For example, we find that, with $\varepsilon = \lambda_{131} = 0.1$, in the best cases (e.g., $m_A^0 = 600$ GeV and $t_\beta = 3$) the shift $|A_{FB(W)}^{SM} - A_{FB(W)}^{RPV}|$ is at the level of a few percent at most in a rather small $|m_{sv}^+ - \sqrt{s}|$ interval of several GeV.

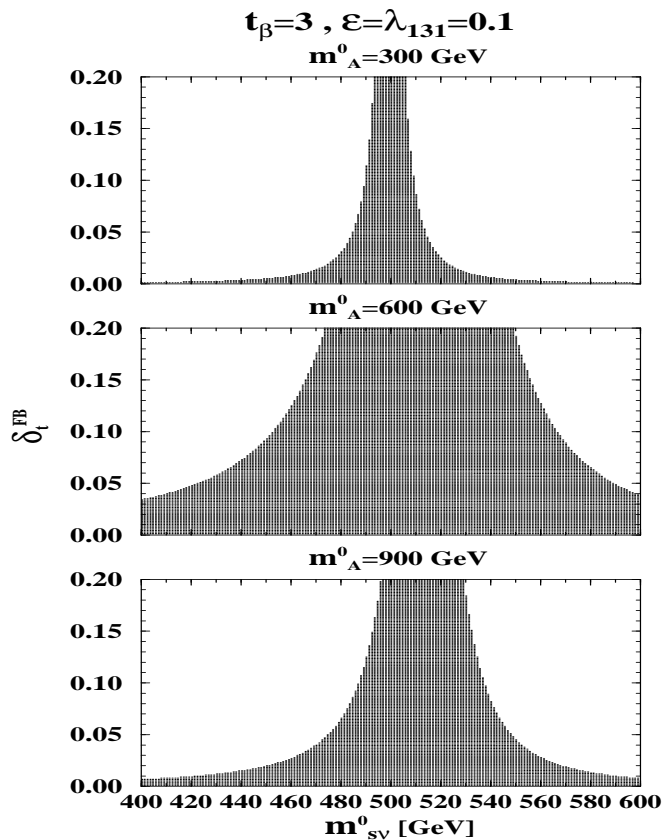


FIG. 10. The shaded areas in the $\delta_i^{FB} - m_{sv}^0$ plane represent values of m_{sv}^0 , that can be excluded for a given experimental error δ_i^{FB} in the actual measurement of the FB asymmetry in $e^+e^- \rightarrow t\bar{t}$ at a 500 GeV e^+e^- collider. This is shown for $\varepsilon = \lambda_{131} = 0.1$, $t_\beta = 3$ and for $m_\Lambda^0 = 300$, 600 or 900 GeV.

VI. SUMMARY AND CONCLUDING REMARKS

We have investigated a SUSY scenario in which lepton number is violated in the scalar potential through a bilinear soft breaking term (RPVBT) as well as in the superpotential through a Yukawa-like RPV trilinear operator (RPVTT). The RPVBT gives rise to mixings between the Higgs and the slepton fields and the new mass eigenstates of the neutral scalar sector are sneutrino–Higgs admixtures.

We considered the case of small lepton number (or R-parity) violation in the sense that all lepton number violating couplings are typically at least an order of magnitude smaller than their “matching” lepton number conserving couplings in the R-parity conserving (RPC) SUSY Lagrangian. In particular, we have used dimensionless R-parity violating (RPV) couplings scaled to the typical RPC couplings, and let these dimensionless couplings be $\ll 1$.

We have carried out a detailed analysis of the CP-even and CP-odd sneutrino–Higgs mass matrices in the presence of a lepton number violating bilinear term in the SUSY scalar potential. We have investigated their behavior under some limiting cases such as small bilinear lepton number violating coupling, a heavy Higgs spectrum and large $\tan^2 \beta$. Also, we have derived Feynman rules for interaction vertices involving the new scalar mass-eigenstates in the theory.

We then suggested that this small lepton number violating SUSY framework may lead to new observable resonance formations in scattering processes that are absent in RPC SUSY and in the “usual” RPV SUSY models in which scalar resonances can occur via the trilinear Yukawa-like RPV interactions in the superpotential. In particular, we focused on two particularly interesting channels, $e^+e^- \rightarrow VV$, $V = Z$ or W and $e^+e^- \rightarrow t\bar{t}$. The resonance structure in these two channels arises only if there are mixings between the sneutrino and Higgs states such that the sneutrino component of the sneutrino–Higgs admixtures couple to the incoming electron beams through Yukawa-like trilinear RPV interactions, while the Higgs component couples to the massive gauge-bosons or to the top quarks. This makes the VV and $t\bar{t}$ production channels unique as compared for example to down-quark and charged lepton pair production in which the RPV s -channel resonances occur via Yukawa-like trilinear RPV interactions on both

vertices. Such resonance signals in $e^+e^- \rightarrow VV$ and $e^+e^- \rightarrow t\bar{t}$ may, therefore, serve as an efficient and direct probe of the RPVBT in the SUSY scalar potential.

We found that the sneutrino-like scalars are expected to yield a dominant resonance effect in both $e^+e^- \rightarrow VV$ and $e^+e^- \rightarrow t\bar{t}$, and that the $t\bar{t}$ channel is much more sensitive to the lepton number violating soft bilinear term. Indeed, we have shown that such a sneutrino-like resonance signal in $e^+e^- \rightarrow t\bar{t}$ is expected to yield significant deviations in observables associated with top-quark pair production which, under favorable circumstances, can be detected in a 500 GeV e^+e^- collider within a 100 GeV sneutrino mass range around the c.m. energy, either via “simple” event counting or via an analysis of the Forward-Backward asymmetry.

If such a resonance will be observed in $e^+e^- \rightarrow t\bar{t}$, then additional measurements should be carried out in the VV production channels as a cross-check for the existence of bilinear lepton number violation in the SUSY scalar potential since the later are expected to yield similar resonance signals. The fact that the same resonance formation is expected to emanate in two different scattering processes will help decipher the nature of these resonance signals.

In the same vein, we have also considered the case that no such resonance enhancement is or will be seen in existing and in future collider experiments. First, we have used the recent LEP2 measurements of the ZZ and W^+W^- production cross-sections to place direct limits on the RPV SUSY parameters involved in this scenario. Also, since this sneutrino–Higgs mixing effect changes the theoretical prediction for the mass of the light SUSY Higgs particle h , we have exploited the recent LEP2 bounds on the h mass to derive further limits on the same lepton number violating SUSY parameters. We found that the two independent LEP2 measurements are complementary for placing limits on these RPV parameters and that they together exclude a significant portion of the relevant SUSY parameter space involved.

In addition we have investigated the expected limits that can be placed on this RPV SUSY scenario in a future 500 GeV e^+e^- collider in the case that no such resonance enhancement are detected in $e^+e^- \rightarrow t\bar{t}$.

Acknowledgements: G.E. thanks the U.S.-Israel Binational Science Foundation, the Israel Science Foundation and the Fund for Promotion of Research at the Technion for partial support.

-
- [1] For reviews of R-parity violation see e.g., D.P. Roy, Pramana, J. Phys. **41**, S333 (1993); G. Bhattacharyya, Nucl. Phys. **B** (Proc. Suppl.) **52A**, 83 (1997); H. Dreiner, in *Perspectives in Supersymmetry*, edited by G.L. Kane (World Scientific, Singapore, 1998), hep-ph/9707435; P. Roy, hep-ph/9712520, Published in *Seoul 1997, Pacific particle physics phenomenology*, 10-17, talk given at APCTP Workshop: Pacific Particle Physics Phenomenology (P4 97), Seoul, Korea, 31 Oct - 2 Nov 1997.
- [2] J. Rosiek, Phys. Rev. **D41**, 3464 (1990), unpublished Erratum in, hep-ph/9511250.
- [3] We follow the notation in Y. Grossman and H.E. Haber, Phys. Rev. **D59**, 093008 (1999).
- [4] S. Roy and B. Mukhopadhyaya, Phys. Rev. **D55**, 7020 (1997); M.A. Diaz, J.C. Romao and J.W.F. Valle, Nucl. Phys. **B524**, 23 (1998); C.-h. Chang and T.-f. Feng, hep-ph/9908295; B. Mukhopadhyaya and S. Roy, Phys. Rev. **D60**, 115012 (1999).
- [5] S. Davidson, M. Losada and N. Rius, Nucl. Phys. **B587**, 118 (2000).
- [6] See e.g., S. Dimopoulos and L.J. Hall, Phys. Lett. **B207**, 210 (1988); V. Barger, G.F. Giudice and T. Han, Phys. Rev. **D40**, 2987 (1989); H. Dreiner and S. Lola, in Munich/Annecy/Hamburg 1991, Proceedings of “ e^+e^- collisions at 500 GeV”, pages 707-711; J. Erler, J.L. Feng and N. Polonsky, Phys. Rev. Lett. **78**, 3063 (1997); J. Kalinowski *et al.*, Phys. Lett. **B406**, 314 (1997); M. Acciarri *et al.* (L3 collaboration), Phys. Lett. **B414**, 373 (1997); S. Bar-Shalom, G. Eilam and A. Soni, Phys. Rev. Lett. **80**, 4629 (1998); J.L. Feng, J.F. Gunion and T. Han, Phys. Rev. **D58**, 071701 (1998); D. Choudhury and S. Raychaudhury, hep-ph/9807373; J. Kalinowski, hep-ph/9807312; T.G. Rizzo, Phys. Rev. **D59**, 113004 (1999); T.G. Rizzo, hep-ph/9907344; S. Lola, hep-ph/9912217; G. Moreau, Ph.D. Thesis, hep-ph/0012156.
- [7] J. Ferrandis, Phys. Rev. **D60**, 095012 (1999).
- [8] See e.g., H.-P. Nilles and N. Polonsky, Nucl. Phys. **B484**, 33 (1997); B. Mukhopadhyaya and S. Roy, Phys. Lett. **B443**, 191 (1998); M. Bisset *et al.*, Phys. Rev. **D62**, 035001 (2000); M. Hirsch *et al.*, Phys. Rev. **D62**, 113008 (2000);
- [9] S. Davidson and M. Losada, hep-ph/0010325.
- [10] Y. Grossman and H.E. Haber, hep-ph/0005276.
- [11] See e.g., F. de Campos *et al.*, Nucl. Phys. **B451**, 3 (1995); A. Akeroyd *et al.*, Nucl. Phys. **B529**, 3 (1998).
- [12] See e.g., K. Choi, E.J. Chun and K. Hwang, J. Math. Phys. **42**, 130 (2001).

- [13] S. Bar-Shalom, B. Mele and G. Eilam, Phys. Lett. **B500**, 297 (2001).
- [14] See e.g., J.F. Gunion, H.E. Haber, G. Kane and S. Dawson, *The Higgs Hunter's Guide* (Addison-Wesley, New York, 1990).
- [15] See J. Erler, J.L. Feng and N. Polonsky in Ref. [6].
- [16] J.F. Gunion and H.E. Haber, Nucl. Phys. **B272**, 1 (1986), Erratum-*ibid.*, **B402**, 569 (1993).
- [17] A. Djouadi *et al.*, Z. Phys. **C74**, 93 (1997).
- [18] S. Heinemeyer, W. Hollik and G. Weiglein, hep-ph/0002213.
- [19] Y. Grossman and H.E. Haber, Phys. Rev. Lett. **78**, 3438 (1997); M. Hirsch, H.V. Klapor-Kleingrothaus and S.G. Kovalenko, Phys. Lett. **B398**, 311 (1997); see also Refs. [3], [5] and [9].
- [20] See S. Bar-Shalom, G. Eilam and A. Soni in Ref. [6].
- [21] See e.g., talk given by Tom Junk at the "LEP Fest", 10 October 2000, in <http://lephiggs.web.cern.ch/LEPHIGGS/talks>.
- [22] S. Bar-Shalom, G. Eilam and A. Soni, Phys. Rev. **D59**, 055012 (1999).
- [23] See summary notes and talks given by Salvatore Mele and Anne Ealet in http://lepww.web.cern.ch/lepww/talks_notes. See also, plots for the Summer 2000 conferences in <http://lepewwg.web.cern.ch/LEPEWWG/plots/summer2000>.